P

PSYCHOPHYSICAL AND NEUROPHYSIOLOGICAL CONSIDERATIONS IN THE DESIGN OF A COCHLEAR PROSTHESIS

Audiol. Ital. 1, 77-117, 1984

PSYCHOPHYSICAL AND NEUROPHYSIOLOGICAL CONSIDERATIONS IN THE DESIGN OF A COCHLEAR PROSTHESIS

M. W. WHITE

Psychophysical and neuropsychophisical considerations in the design of of a cochlear prosthesis.

The Authors carry out an analysis of threshold, loudness and intensity discrimination functions for a wide range of stimuli. Phenomenological models of these functions are developed and neurophysiological concepts, such as temporal integration processes, are used to interpret the behavioural data presented. Comparative data are presented for single and multichannel prostheses in order to provide the designer with a more effective understanding of the consequences of electrical stimulation of the auditory nerve.

KEY WORDS: Behavioral threshold, cochlear prosthesis, stimulation of auditory nerve.

Introduction

Direct electrical stimulation of surviving auditory nerve fibers or ganglion cells is now being employed to restore some aspects of hearing in profoundly deaf patients (Simmons, 1964; Hochmair, 1980; Fourcin *et al.*, 1979; Tong, 1979; Merzenich, 1973). Psychophysical studies of the sensations of such patients has indicated that presumably localized activation of groups of fibers from a given area of the basilar membrane gives rise to « auditory » sensations. In general, the magnitude of these sensations increases with stimulus amplitude. In this study we examine in detail threshold, loudness, and intensity discrimination functions for a wide range of stimuli. Phenomenological models of these functions are developed and neurophysiological concepts are used to interpret the behavioral data presented. The purpose of this study is to develop a set of conceptual « tools » that will allow the prosthesis designer to more effectively understand the consequences of electrical stimulation of the auditory nerve. It is hoped that the use of this knowledge will help us design more effective auditory prostheses.

This study draws a great deal from the work of others in the fields of neurophysiology and psychophysics. Many concepts developed by these investigators will be applied to the interpretation of the data to be presented here. Studies of cochlear nerve responses to electrical stimuli have been reported by Kiang and Moxon (1972). These authors compared eighth nerve firing patterns to a limited set of both electrical and acoustic stimuli. Firing rates as a function of stimulus intensity and threshold as a

School of Medicine, Department of Otolaryngology University of California, San Francisco, California 94243, U.S.A.

Lavoro presentato al Premio Internazionale di Audiologia « Stelio Crifò ».

function of frequency were defined. Phase-locking of responses evoked by a 200 Hz sinusoidal electrical stimulus was also studied by Kiang and Moxon (1972). Clopton *et al.* (1980) have studied threshold and dynamic ranges for different stimulating electrode configurations and waveforms. Frankenhaeuser and Huxley (1964), McNeal (1976), and Teicher and McNeal (1978) have developed general models describing the electrical excitation of myelinated nerve fibers such as those which comprise the predominant afferent population in the auditory nerve. See Loeb *et al.* (1983) for a discussion of the biophysics of intracochlear electrical stimulation of these neurons.

The primary goal of this research is to better understand how we can utilize electrical stimulation of the auditory nerve to help the totally deaf to communicate. In this study, the communication (via the cochlear implant) of information related to the intensity of the stimulus is examined. This work is intended to aid the design of both multi-channel and single channel cochlear prosthesis. In a single or multi-channel cochlear prosthesis we must at least minimally understand how to generate stimuli that are audible, not too loud, and that allow the subject to discriminate differences in stimulus intensity. This study was designed to enable the developers of such prosthetic systems to understand many of the basic principles necessary to generate electrical stimuli that meet these requirements. This study is particularly useful in that data for a *large* range of stimuli are presented.

Goals of Cochlear Prosthesis Research

A sound processor should minimally be capable of « adjusting » the amplitude of the stimulus such that the stimulus remains within the dynamic range of the subject and yet does not so restrict amplitude excursions that little or no intensity information is conveyed. Although this should be considered a minimal requirement, and not at all a « sufficient » requirement, it is not readily achieved. Indeed, many current processors do not meet this minimal requirement. The exact placement of the stimulus within the dynamic range is a further refinement of a processor's design specification. Both intensity descrimination functions and loudness functions have been suggested in determining the placement of the stimulus within the dynamic range.

We designate the highest stimulus level that is still comfortable to the subject as the « maximum comfortable loudness level » or simply « MCL ». Threshold and MCL are very important functions, for they define the widest possible limits of audible and tolerable stimulation. We define the ratio of these two limits as the subject's « dynamic range ». The ratio is most often expressed in dB.

Threshold, maximum comfortable loudness (MCL), and dynamic range functions have been measured for biphasic pulse stimuli. For comparison, some sinusoidal stimuli were also investigated. Pulsatile stimuli were primarily used in these studies.

Pulse width can be varied independently of the pulse frequency. Pulse width is defined as the *total* duration of the biphasic pulse. With sinusoidal stimulation the duration of a sinusoidal cycle varies inversely with the frequency of stimulation. In contrast, with pulsatile stimulation, these two variables can be varied independently of each other. Furthermore, pulse width and pulse frequency (i.e. pulse rate) have distinctly different effects when considered in terms

of the most common types of neural excitation models.

Models of neural excitation

In order to describe and interpret the data to be presented, it is useful to review several models of threshold to electrical stimulation that may be useful in the interpretation of the data. One of the simplest behavioral threshold models incorporates a model of neural membrane excitation. In using neural membrane models to approximate behavioral threshold functions, a number of assumptions are often invoked. It is assumed that the medium between the stimulating electrodes and the excitable membrane acts only as a purely resistive attenuator (Spellman, 1982). It is also assumed that the stimulator is an ideal current source (Vurek *et al.*, 1981). If this later assumption is approximately valid, there will be little effect on neural threshold due to nonlinear and frequency dependent electrode impedance. Other assumptions are commonly made about the relationship between behavioral threshold and the excitation of nerve fibers. For example, a working assumption might be that behavioral threshold occurs when « N » neural discharges have been elicited within a given time window, from one or more fibers. For example, if there is no spontaneous activity and the threshold detector is ideal, only one action potential would be necessary to elicit behavioral threshold.

Hill's model (Hill, 1936) is schematically depicted in figure 1. The stimulator is represented by the current source. The passive membrane capacitance and resistance are represented by the capacitor « Cm » and the resistor « Rm » in parallel. Accomodative effects are approximated by the capacitor « Ca » and the resistor « Ra » in series. The voltage across « Ra » is monitored by the « threshold voltage detector ». When the voltage across this resistor goes above a present threshold voltage « Vt », the detector generates a simulated action potential. This model mimicks certain general features of neural excitation. For example, the model predicts that a monophasic pulse will elicit an action potential if the *charge* within the pulse is above some fixed threshold value and if the pulse width is sufficiently within the time constant of the membrane (tm=CmRm). Likewise, at the higher sinusoidal stimulus frequencies, this

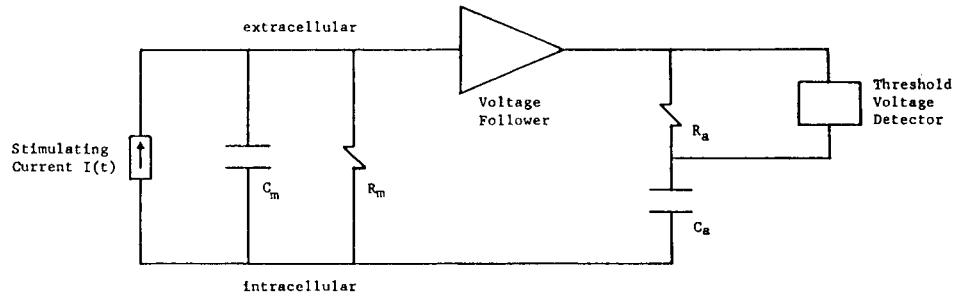

Fig. 1. - Hill's lumped circuit neural excitation model.

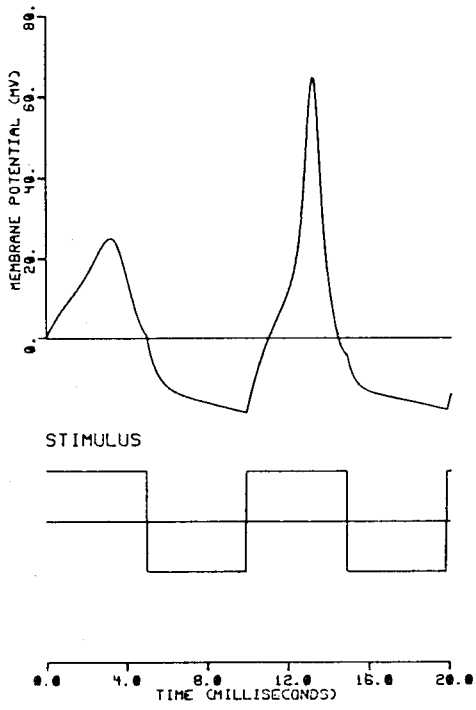

Fig. 2.

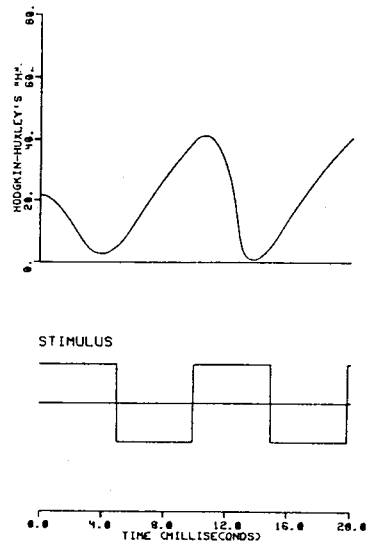

Fig. 3.

Fig. 2. - Simulated membrane potential as a function of time for a square wave stimulus initiated at t=0. The stimulus waveform is displayed on the same time scale as that for the membrane potential function. A modified Hodgkin-Huxley model was used in this simulation. Beta-h was increased by a factor of four over that in the H-H model.

Fig. 3. - Hodgkin-Huxley variable « h » as a function of time for a square wave stimulus initiated at t=0. The stimulus waveform is displayed on the same time scale as that for the Hodgkin-Huxley state variable « h ». A modified Hodgkin-Huxley model was used in this simulation. Beta-h was increased by a factor of four over that in the H-H model.

model predicts that threshold will increase at a rate of 6 dB/oct as the sinusoidal stimulus frequency is increased. The model also predicts another commonly observed phenomenon: that threshold is never reached if a stimulus ramp rises at too slow a rate. In the model, this is due to « Ra » and « Ca », which represent accomodative phenomena. For sinusoidal stimulation, accomodation is evident at the lower frequencies (below 50-100 Hz), where the threshold no longer decreases as the frequency is decreased.

Hill's model is a useful starting point for describing and understanding certain aspects of neural excitation. However, other aspects of neural excitation are not well represented by Hill's model. For example,

Hill's model does not simulate any post-excitatory phenomena. Hill's model is primarily a linear model. It is non-linear only in its use of the « voltage threshold detector ». More complicated, non-linear models such as the Hodgkin-Huxley model (H-H model) and the Frankenhauser-Huxley model (F-H model) more accurately represent neural excitatory behavior (Frankenhauser and Huxley, 1964). These models simulate many more features of neural responses than does Hill's model. Two of these features are discussed below: (1) sensitization due to prior hyperpolarization of the membrane; and (2) temporal integration of sub-threshold, charge-balanced stimuli.

Sensitization due to prior hyperpolarization of the membrane

Figure 2 illustrates one feature of neural excitation. If one phase of the stimulus hyperpolarizes the neural membrane, the membrane may become more sensitive to the stimulus subsequent to this hyperpolarization. A modified Hodgkin-Huxley model (1952) was used for this simulation. The first depolarizing phase does not excite the model nerve. However, after the hyperpolarizing phase of the stimulus. In this example, both the hyperpolarizing phase and the subsequent depolarizing phase were necessary to excite the model nerve at this stimulus level. Figure 3 displays how the Hodgkin-Huxley variable « h » (i.e. the sodium deactivation variable) varies during the stimulation. As « h » increases, the excitability of the membrane increases. The value of « h » increases to a higher value during and shortly after the hyperpolarizing phase, than its maximum value during the first phase of depolarization. This simulation illustrates how a nerve membrane become more sensitive after a hyperpolarizing stimulus. The duration of the hyperpolarization phase is critical in determining how effective it is in increasing the nerve's sensitivity. Generally, if the hyperpolarizing phase is too short or too long the nerve's excitability will not be increased. The graph in figure 4 was constructed using the same nerve membrane model used in the previous example. The model is identical to the H-H model; except that « beta h » has been increased by a factor of four. This has the effect of increasing the rate of response of the deactivation variable « h ». The graph in figure 4 was constructed by determining the relative current level at which a simulated action potential was generated for a set of frequencies. Figure 5 indicates how many stimulus cycles were necessary to excite the model membrane at threshold current levels. Over the limited frequency range illustrated, this model approximates some of the behavioral threshold features observed. The major effect on the nerve's « frequency response » is the increased slope (i.e. greater than the Hill model's 6 dB/octave) over the 90 to 200 Hz frequency region.

A note of caution should be inserted here. Such highly nonlinear simulation models can be used to generate a relatively wide range of behavior by adjusting the model's parameters. Therefore, a very good « curve-fit » could be achieved on relatively complex functions even though the actual mechanism(s) is not at all related to the simulation model used.

Temporal Integration at the Nerve Membrane

Figure 6 (from Butikopfer and Lawrence, 1979) illustrates « temporal summation » at the simulated nerve membrane

(simulated with an F-H model). Butikopfer and Lawrence (1979) also present empirical evidence from a study of the electrical stimulation of mylenated nerve fibers that corroborates their simulations using the F-H model. In their F-H model simulation, the membrane voltage does not return to zero after each charge-balanced biphasic pulse. Each biphasic pulse increases the depolarization of the membrane. The F-H model predicts that closely-spaced biphasic pulses would be more effective at exciting the nerve than just one biphasic pulse. In contrast, Hill's model predicts that multiple charge-balanced biphasic pulses would be no better at exciting the nerve than just one pulse.

The simulations of membrane hyperpolarization and temporal integration may offer insights useful for interpreting the psychophysical data to be presented.

Research strategy

This paper is divided in two sections. The first section describes the behavior of threshold and MCL functions for a wide range of stimuli. Threshold and MCL functions delineate the extremes of the subject's dynamic range. The second section deals with the mid-range functions of intensity discrimination and loudness. The experiments were designed to help us develop phenomenological models (and in some cases, evidence for specific mechanisms) useful in understanding the subjects responses to a wide range of stimuli. Certain stimuli were particularly useful in separating

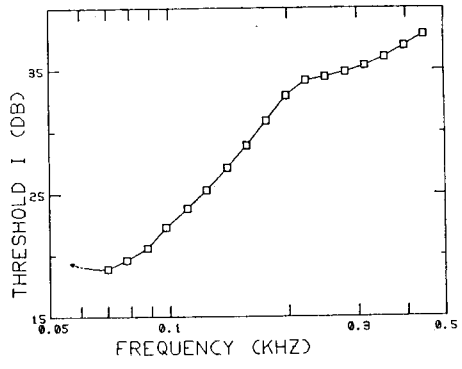

Fig. 4.

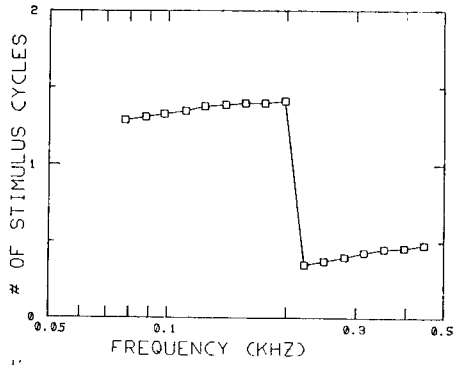

Fig. 5.

Fig. 4. - Neural threshold to membrane excitation as a function of sinewave stimulus frequency using a model membrane simulation. A modified Hodgkin-Huxley model was used in which beta-h was a factor of four greater than that in the original Hodgkin-Huxley membrane model. The sinusoidal stimulus was initiated at a zero crossing with the first phase depolarizing the membrane model. The first phase of the sinusoidal stimulus depolarized the simulated membrane.

Fig. 5. - This graph displays the point in time at which an action potential was generated in the simulation represented by figure 4. Time of occurance was recorded in terms of the time that the membrane voltage reached 90% of maximum. « Time of occurance » was normalized by dividing the actual time at which an action potential occured by the period of the sinewave stimulus.

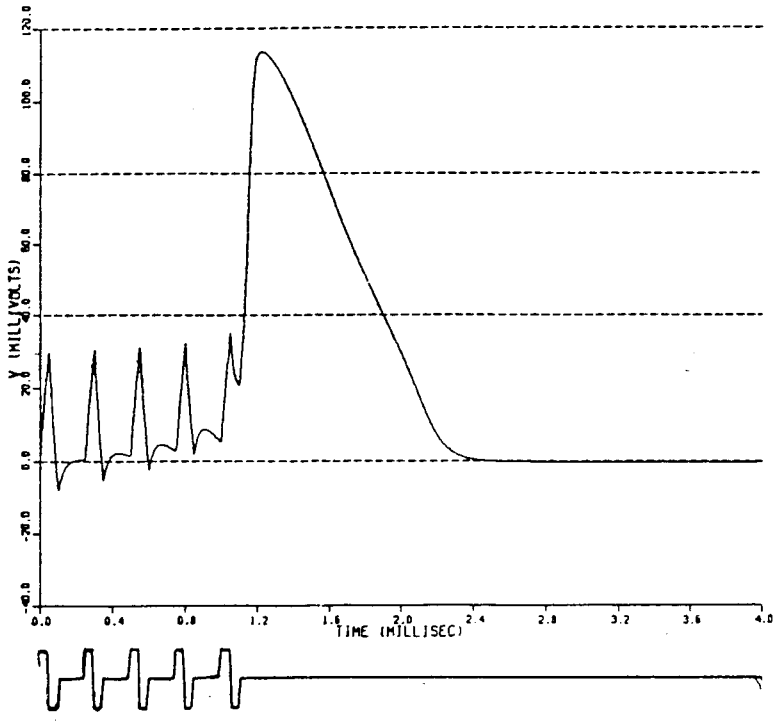

Fig. 6. - Simulated membrane voltage as a function of time for multiple biphasic pulse stimuli. The Frankenhauser-Huxley model was used in this simulation. Figure courtesy of Butikopfer and Lawrence (1979).

the effects of two or more mechanisms. For example, single biphasic pulse and single sinusoidal cycle stimuli were used to obtain threshold and MCL functions that were substantially unaffected by temporal integration mechanisms. By comparing threshold and MCL functions for single pulses with those for multipulse stimuli, the significance contribution of any temporal integration mechanism(s) was estimated. If the threshold or the MCL function for multiple charge-balanced biphasic pulses was significantly lower than those for single pulses, some form (peripheral and/or central) of temporal integration was likely responsible.

Methods

Thresholds were measured with a modified Békésey tracking procedure using a minimum of 6 threshold crossings for each threshold estimate. The average of the stimulus minima and maxima was computed to determine the estimated threshold stimulus current. The subject pressed a button when he or she heard the stimulus and released the button when the stimulus was no longer audible. 600 milliseconds elapsed between the end of a stimulus burst and the onset of the next stimulus burst.

The maximum comfortable loudness level was determined by initiating the stimulus at an amplitude slightly above threshold and gradually increasing the stimulus level on a linear amplitude scale until the subject pressed a button to indicate that the stimulus had reached the « maximum comfor-

table loudness ». The computer-generated stimulus sequence was then immediately halted and the next « MCL » series initiated after a three second delay. 600 milliseconds elapsed between the end of a stimulus burst and the onset of the next stimulus burst.

Intensity discrimination was measured with a 2A-2IFC adaptive procedure which converged to a 70.7% correct level. If the subject made two correct responses in a row, the discrimination task was made more difficult. For every incorrect response, the task was made less difficult. A light marked each interval in the two interval task. At least eight threshold crossing occurred before the intensity dl was calculated. The first two threshold crossing were not used in the calculation of the estimated intensity dl. This adaptive procedure was described by Levitt (1970).

During all tests, the subject could immediately terminate stimulation by disengaging a « master » switch which would immediately disconnect all electrodes from the optically-isolated current drivers (Vurek, 1981). In addition, the computer-generated stimulus program utilized a set of on-going « consistency checks » which verified that the system components were operating properly. If any one of these « consistency checks » proved invalid, stimulation immediately ceased within 1 msec or less.

All stimuli were generated with an optically-solated, controlled current source (Vurek, 1981) and delivered directly to the subject's electrode contacts via a subcutaneous cable. This cable excited through the skin and was connected through a set of relays to the described stimulators. Stimuli were generated from a digital-to-analog converter at a sampling rate of 20 KHz. Both pulsatile and sinusoidal stimuli were generated. Where appropriate, an anti-aliasing filter was utilized.

Subjects were implanted with scala tympani intracochlear electrode arrays of sixteen wires. The electrode array and the implantation procedure are described in detail in Loeb et al., 1983. The apical-most electrode is inserted approximately 21 to 26 mm into the scala. Each electrode contact is mushroom shaped in order to increase its surface area. The eight bipolar electrode pairs are spaced at 2 mm intervals along the silastic intracochlear insert. The inter-contact spacing between bipolar pairs is approximately 700 microns, center-to-center. The electrode pairs are oriented approximately radially relative to the axis of the cochlea. Electrode numbering begins at the apical-most part of the array and progresses basally, such that the apical-most bipolar pair is labeled « (1, 2) » and the basal-most bipolar pair is labeled « (15, 16) ». An odd numbered electrode represents an electrode contact placed more towards the modiolus. Both monopolar electrode configurations as well as bipolar electrode configurations were used in this study. In the monopolar configuration, only one electrode contact was stimulated and the « return » path was an ear-clip located on the ear lobe nearest the implanted cochlea. With monopolar stimulation, the same numbering system is used, but only one number displayed to indicate which electrode contact is stimulated.

Subject A, age 60, had a gradual onset of hearing loss starting after age 10 gradually increasing until her loss was profound about thirty years later. There is no family history of deafness nor any other known reason for this subject's hearing loss.

Subject B, age 61, had a gradual onset of hearing loss after measles at age 8 gradually increasing until the loss was profound in her twenties. Both subjects A and B participated in tests over a three to four month period.

Subject C, age 51, had a sudden loss of hearing after an automobile accident (at age 20) in which he sustained a bilateral fracture. Subject C underwent psychophysical and speech testing over a period of approximately a month and a half.

All subjects exhibited greater than 110 dB loss across the frequency range. All subjects were post-lingual. Each of the three subjects was unable to utilize even specialized high-power body *hearing*-aids in standard speech discrimination tests. A thorough psychological evaluation was conducted to estimate how the subjects would respond to consequences of the implantation.

Results

Responses to single pulses and cycles

Figure 7 illustrates threshold and MCL responses as a function of pulse width for single biphasic pulses. The slope of the threshold function significantly increases for

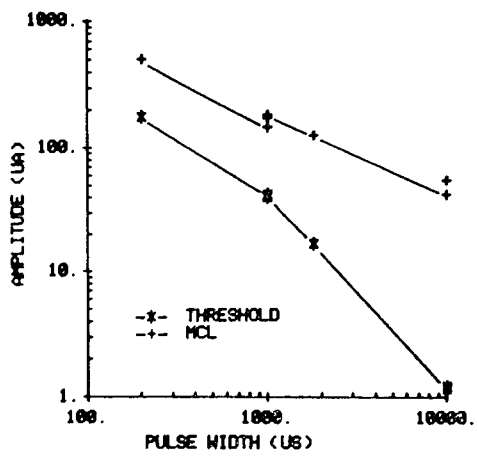

Fig. 7.

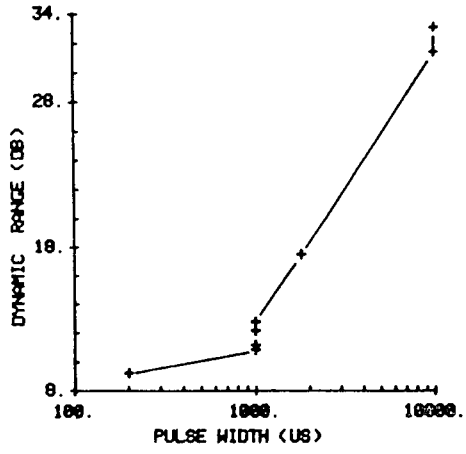

Fig. 8.

Fig. 7. - Threshold and MCL for single pulses as a function of pulse width. Data from subject B with bipolar electrode pair (7, 8) stimulated.

Fig. 8. - Dynamic range (derived from data in figure 7) for singel pulses as a function of pulse width. Data from subject B with bipolar electrode pair (7,8) stimulated.

pulse widths greater than 1000 μsec (going from a 4-6 dB/octave slope to an approximately 9 dB/octave slope function, whereas the slope of the MCL function remains relatively constant and less steep as a function of pulse width.

Figure 8 illustrates how the dynamic range changes as a function of pulse width for single biphasic pulses. The dynamic range is quite narrow (8-12 dB) for pulse widths of 200 to 1000 μsec, but increases very significantly at the larger pulse widths. At a pulse width of 10 msec (i.e. a pulse width comparable to the duration of a cycle of a 100 Hz sinusoidal stimulus) the dynamic range is nearly 32 dB. This dynamic range is approximately that of a 300 msec, 100 Hz sinewave stimulus.

Figure 9 displays threshold and MCL (maximum comfortable level) as a function of sinusoidal stimulus frequency. The sinusoidal stimulus was either a burst with a 300 msec duration or a single sinusoidal cycle. The single cycle threshold curve is only approximately represented by a single slope of about 6 dB per octave. Threshold does not increase quite as much as 6 dB/octave at the higher stimulus frequencies. An average increase in threshold of 5 dB/octave over the 1000-4000 Hz range for single cycles is typical. Between 100 and 1000 Hz, the average increase in threshold is 9 dB/octave for single cycles.

The spectrum of single pulses and sine cycles is a very significant function of the pulse width cycle duration. Threshold, MCL, and dynamic range functions are functions of pulse width and as a consequence they are also functions of the spectrum of these stimuli.

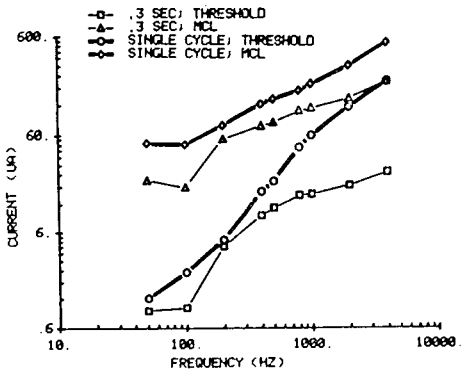

Fig. 9.

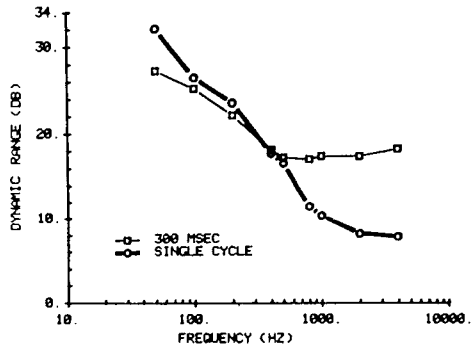

Fig. 10.

Fig. 9. - Threshold and MCL as a function of frequency for single sinewave cycles and a burst, 300 msec in duration. Data is from subject B with bipolar electrode pair (7,8) stimulated. The sinusoidal bursts were generated without onset or offset envelopes.

Fig. 10. - Dynamic range as a function of frequency for single sinewave cycles and a burst duration 300 msec. Data is from subject B with bipolar electrode pair (7,8) stimulated.

Responses to repetitive biphasic stimuli

Responses to multiple cycle sinewave stimuli

As outlined in the strategy of research section (section 5), responses to multiple cycles and pulses have been examined in order to understand the effects of any hypothetical temporal integration processes.

In figure 9, the threshold curve for 300 msec bursts exhibits a relatively flat portion between 50 Hz and 100 Hz and a steep increase in threshold as the stimulus frequency is increased from 100 Hz to 200 Hz. Above 200 to 400 Hz threshold increases at a relatively shallow rate of 3-4 dB per octave. The major difference between the single cycle and 300 msec MCL curves is a small vertical shift. For single cycles, a somewhat larger stimulus amplitude is required to elicit the maximum comfortable loudness.

For the 300 msec stimulus, threshold and MCL curves are roughly parallel for stimulus frequencies above 200 to 400 Hz. As a consequence, the dynamic range (see Figure 10) remains approximately constant for short duration sinusoidal stimuli. ~~Thre longer duration stimulus~~. This is not true for short duration sinusoidal stimuli. Threshold increases at a rate greater than that of ~~As the stimulus frequency is increased, the dynamic range~~ MCL vs frequency over the entire frequency range that was measured (50-4000 Hz). ~~continues to decrease for these short stimuli.~~ The reduction in the dynamic range for these short stimuli, as compared to the approximately constant dynamic range of the 300 msec stimuli, is primarily due to the difference in the shape of the two threshold curves.

Figure 10 is a plot of dynamic range as a function of the stimulus frequency for the data presented in Figure 9. The dynamic

range for short and long duration sinusoids is roughly the same for frequencies below 400 Hz. For frequencies higher than 400 Hz, figure 10 illustrates that the dynamic range for the short duration stimuli is considerably less than that for 300 msec stimulus bursts. Above 400 Hz, the dynamic range for the short duration stimuli is considerably less than that for 300 msec stimulus bursts. Above 400 Hz, the dynamic range remains approximately constant at about 17 to 18 dB for the 300 msec bursts. However, for the single cycle sinusoids, the dynamic range decreased from about 18 dB at 400 Hz to less than 8 dB at 4 KHz. Such changes in dynamic range as a function of stimulus duration can have a profound effect on speech processing strategies.

The differences in the two threshold functions is the primary cause of the large differences in the dynamic range for the two types of stimuli. Threshold functions for 300 msec sine bursts are quite different than threshold functions for single cycles, probably because of one or more temporal integration mechanisms.

Responses to multiple pulses

Graph 11 illustrates how threshold current changes as the number of pulses increase. As the number of pulses increase the threshold decreases. The greatest change in threshold occurs at the shorter interpulse intervals; particularly for interpulse durations less than 5 msec. For example, the 1 msec inter-pulse interval curve exhibits a

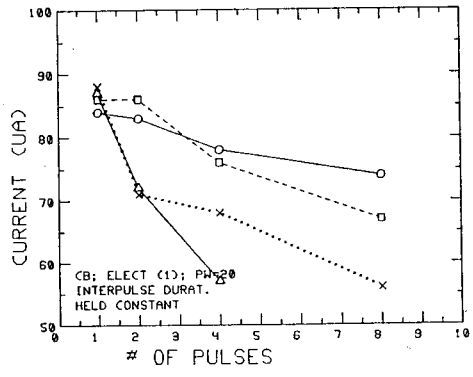

Fig. 11.

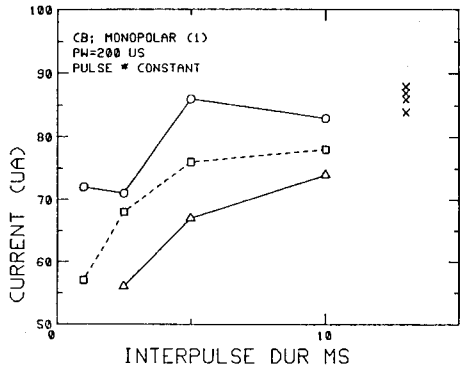

Fig. 12.

Fig. 11. - Threshold current as a function of the number of 200 usec biphasic stimulus pulses. Data is from subject B with monopolar electrode (1) stimulated. Circles represent thresholds to pulses with an inter-pulse delay of 10 msec. Squares represent thresholds to pulses with an inter-pulse delay of 5 msec; X's 2.5 msec; Δ - 1 msec.

Fig. 12. - Threshold current as a function of the inter-pulse duration (i.e., inter-pulse) delay in msec. Pulses were biphasic and 200 μsec in duration. Data is from subject B with monopolar electrode (1) stimulated. Circles represent stimuli with two pulses. Squares represent stimuli with four pulses. Triangles represent stimuli with eight pulses. The X's represent stimuli with only one pulse.

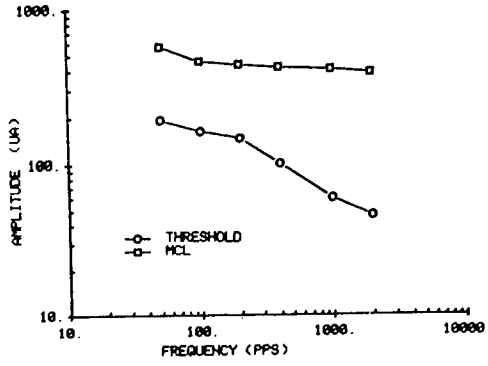

Fig. 13.

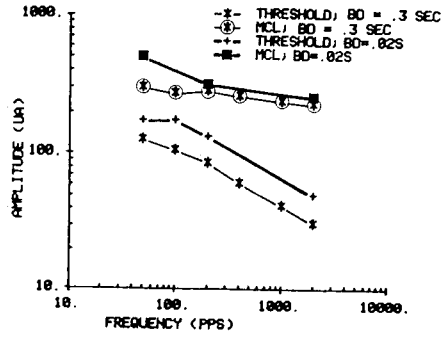

Fig. 14.

Fig. 13. - Threshold and MCL as a functin of pulse rate for pulse trains 300 msec in duration and pulse widths of 200 usec. Data is from subject B with bipolar electrode pair (15, 16) stimulated.

Fig. 14. - Threshold and MCL as a function of pulse rate for pulse trains of 20 msec and 300 msec in duration and a pulse width of 200 usec. Data is from subject B with bipolar electrode pair (7, 8) stimulated.

very large decrease in threshold as the number of pulses is increased. In contrast, the thresholds of pulse trains with 10 msec inter-pulse intervals exhibit only small decreases as the number of pulses is increased.

Figure 12 is derived from the same data illustrated in figure 11. Threshold is plotted as a function of the inter-pulse duration, with each curve representing a different number of pulses. As the inter-pulse interval increases from 1 msec to 10 msec, the threshold increases. A large increase in threshold occurs as the interpulse delay is increased from 2.5 msec to 5 msec. The curve with highest thresholds represents thresholds obtained with a stimulus of only two, 200 µsec biphasic. The dashed curve represents thresholds with four pulses, and the curve with lowest thresholds is for stimuli of eight pulses. The « X's » in the upper right for graph 12 represent thresholds for single biphasic pulses.

Figure 13 is a plot of threshold and MCL for 200 µsec (100 µsec per phase) biphasic pulse trains applied to two bipolar electrodes (15,16) in subject B. Threshold decreases as a function of pulse rate, particularly from 200-400 to 2000 pps. Stated in other terms, the threshold decreases very significantly for interpulse duration less than 5 msec. In contrast, the MCL function exhibits only a very small decrease slope as the frequency is increased. Figure 14 illustrates a similar function for a 20 msec and a 300 msec stimulus driving bipolar electrode pair (7,8) in subject B.

Figure 15 illustrates how dynamic range increases as a function of pulse rate for the data illustrated in figure 13. Because threshold decreases significantly with pulse rate compared with MCL function, dynamic ran ge increases quite significantly, particularly for pulse rates greater than 200 pps.

Figure 16 illustrates how threshold and MCL vary as a function of burst duration

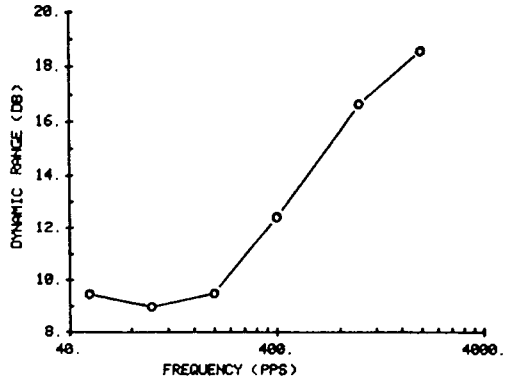

Fig. 15. - Dynamic range as a function of pulse rate for pulse trains 300 msec in duration and pulse widths of 200 usec. Data is from subject B with polar electrode pair (15, 16) stimulated. Derived from data illustrated in figure 9.

for a 2000 Hz sinusoidal stimulus. Threshold decreases at a greater rate than does the MCL function when the burst duration is increased. As a consequence, the dynamic range increases as a function of the burst duration (Fig. 17).

Additional evidence for temporal integration is observed in measures of threshold as a function of burst duration. Figures 18, 19 and 20 illustrate threshold as a function of burst duration. In these illustrations, pulse width was 200 μsec (100 μsec/phase). In two subjects (A and B), thresholds were obtained at 100, 200, 400, and 1000 pps stimulus bursts except in figure 20 where the 200 pps data was not obtained. The greatest change in threshold vs burst duration occurs at the highest frequency (i.e. pulse rate) tested: 1000 pps. At 1000 pps, the greatest change in threshold occurs within the first 20 msec. Because MCL vs burst duration changes relatively little in these two subjects as a function of burst duration, this would imply that the dynamic range changes significantly within the first 20 msec of these stimuli: the dynamic range being at a minimum for the very shortest

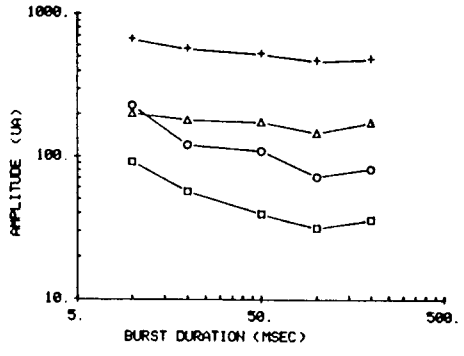

Fig. 16.

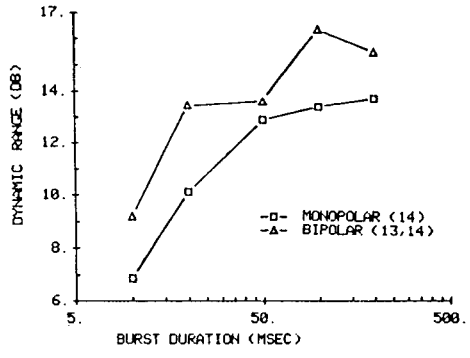

Fig. 17.

Fig. 16. - Threshold and MCL for 2000Hz sinusoidal stimuli as a function of burst duration for a bipolar (13, 14) and a monopolar (14) electrode configuration in subject A.

Fig. 17. - Dynamic range for 2000 Hz sinusoidal stimuli as a function of burst duration for a bipolar (13, 14) and a monopolar (14) electrode configuration in subject A. Derived from data illustrated in figure 16.

burst durations, and increasing considerably within the first 20 msec.

For 100 and 200 pps pulse stimuli only very modest decreases in threshold occur for very large changes in the burst duration. These small threshold changes could be the result of at least ~~two~~ three factors: (1) A central detection mechanism may integrate over a considerable time interval to detect a signal. In the normal auditory system there is strong evidence that a more central temporal integration mechanism operates over at least a 50-100 msec interval; (2) Although most presumed « temporal integration at the nerve » occurs during a 2-5 msec time window, a small but significant peripheral tem-

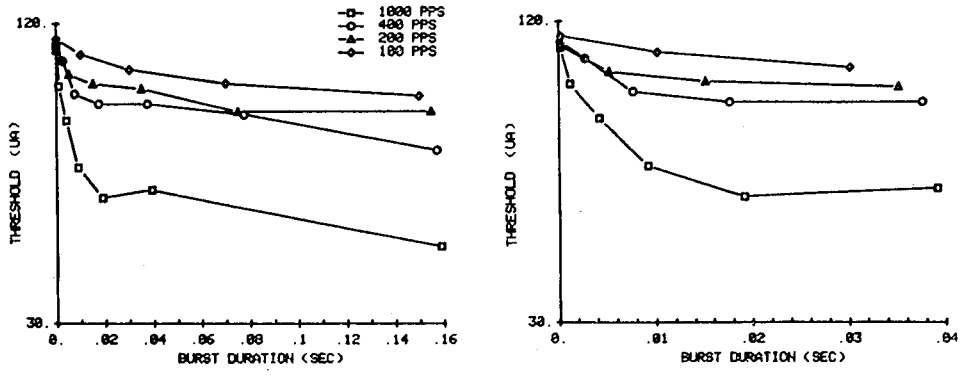

Fig. 18. - Threshold as a function of burst duration for a set of pulse rate rates (100, 200, 400, and 1000 PPS) and a pulse width of 200 μsec. The vertical scale is logarithmic. Data is from subject B with bipolar electrode pair (1, 2) stimulated. A 40 msec and a 160 msec time scale are used to display the data over the full range of measure.

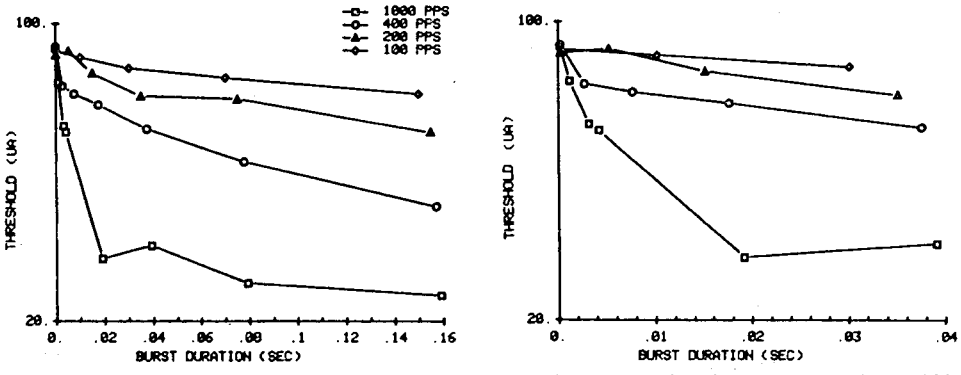

Fig. 19. - Threshold as a function of burst duration for a set of pulse rate rates (100, 200, 400, and 1000 PPS) and a pulse width of 200 μsec. The vertical scale is logarithmic. Data is from subject B with monopolar electrode (1) stimulated. A 40 msec and a 160 msec time scale are used to display the data over the full range of measure.

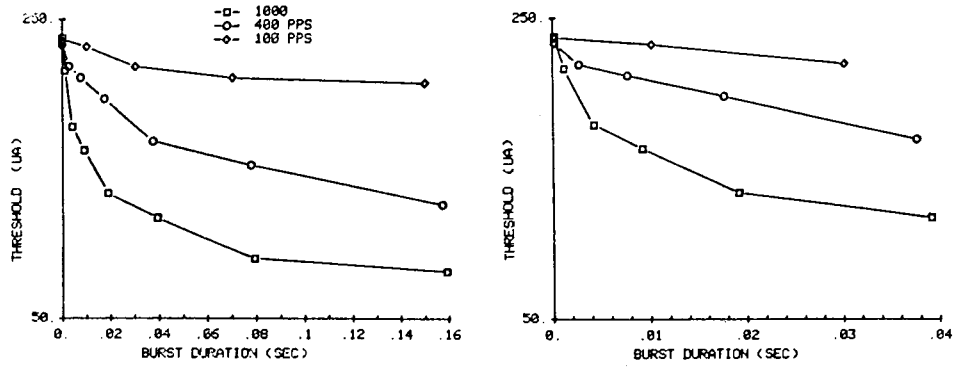

Fig. 20. - Threshold as a function of burst duration for a set of pulse rate rates (100, 200, 400, and 1000 PPS) and a pulse width of 200 usec. The vertical scale is logarithmic. Data is from subject A with electrode pair (1, 16) stimulated. A 40 msec and a 160 msec time scale are used to display the data over the full range of measure.

poral integration might occur over a considerably longer interval; (3) Over the stimulus interval, the extracellular and intracellular ionic concentrations may change, and thereby change the nerve's excitability (Moran and Palti, 1980; White, 1983).

The data for the 400 pps pulse train also exhibits a decline in threshold as the burst duration is increased. In figure 18, the threshold decreases in a manner similar to the 100 and 200 pps pulse trains. However, in figures 19 and 20, the threshold decreases significantly at durations greater than 20 to 40 msec.

Figure 21 illustrates thresholds for bipolar electrodes (1,2) in subject B and also illustrates thresholds for monopolar electrode (1) in the same subject. For 1000 pps stimuli, threshold drops by a factor of about 3.5 during the first 20 msec with monopolar stimulation as compared to only a factor of two for the same interval with bipolar stimulation. If the interpulse duration is less than 2-5 msec, monopolar (as compared to closely-spaced bipolar electrode pairs) stimulation consistently causes a larger percentage decrease in threshold as the burst duration is increased over the first 0-20 msec. Also, threshold declines at a greater rate with monopolar stimulation (as opposed to bipolar stimulation) when the pulse rate is increased above 200-400 pps.

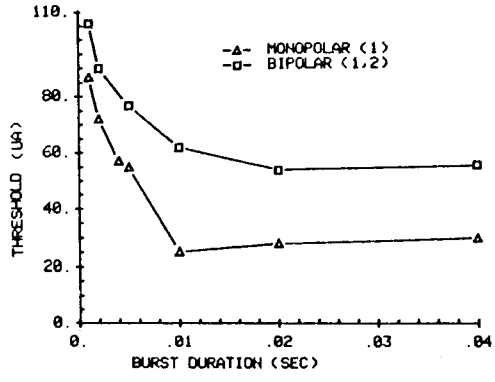

Fig. 21. - Threshold as a function of burst duration for monopolar (1) and bipolar (1, 2) stimulation. Pulse widths of 200 μsec and repetition rates of 1000 PPS were used in these experiments with subject B. Data from figures 18 and 19.

Interaction of pulse width and pulse rate factors

Figure 22 displays dynamic range as a function of the pulse rate and pulse width for biphasic pulse trains. The burst duration of all stimuli was 300 msec. The dynamic range is greatest for larger pulse widths. Also, the dynamic range increases as the pulse rate is increased above 200 pps.

Another significant response feature is evident in figure 22. For pulse widths of 900 and 1800 μsec, the dynamic range at 100 pps is greater than the dynamic range at 50 pps or at 200 pps. This is due to the lower threshold at the 100 pps rate as compared to the thresholds at 50 pps and 200 pps, for pulse widths of 900 and 1800 μsec. Figure 23 illustrates how the threshold dips at 100 pps for the 1800 μs pulse

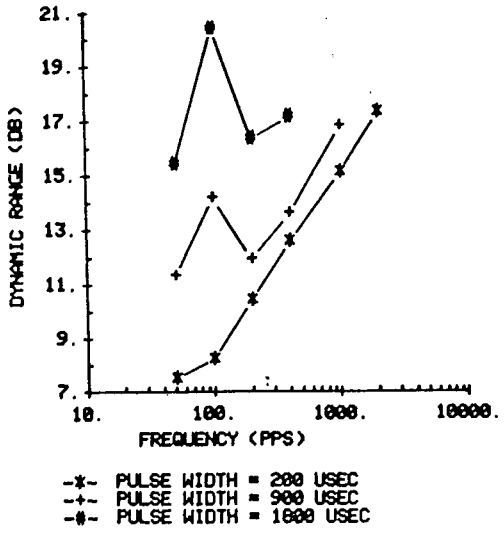

Fig. 22. - Dynamic range as a function of pulse rate and pulse width for pulse trains 300 msec in duration. Data is from subject B with bipolar electrode pair (7, 8) stimulated. Data from that illustrated in figure 23.

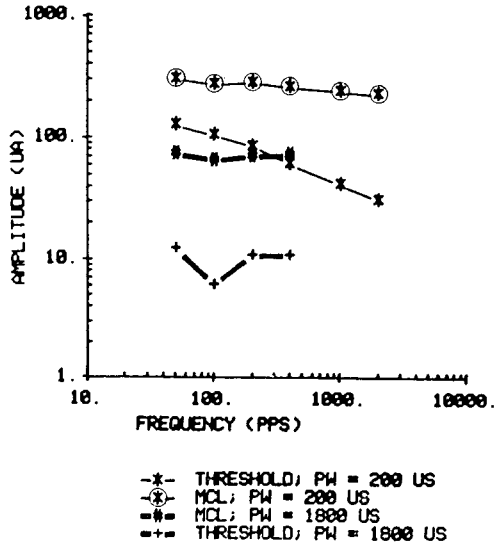

Fig. 23. - Threshold and MCL as a function of pulse rate for pulse trains 300 msec in duration and pulse widths of 200 μsec and 1800 μsec. Data is from subject B with bipolar electrode pair (7, 8) stimulated.

width stimulus, but does not dip when 200 μs pulses are used.

Figures 24 and 25 illustrate how threshold, MCL, and dynamic range change as a function of pulse width for pulse trains of 300 msec in duration and pulse rates of 100, 400, and 1000 pps. Increasing pulse widths consistently extend the dynamic range for these pulse trains; just as in the single pulse case illustrated by figure 7 and figure 8. As previously described, threshold tends to be a decreasing function of pulse rate; most notably for pulse rates above 200 to 400 pps. In figure 24, threshold decreases with increasing pulse rate except at a pulse width of 1800 μsec, where the threshold for the 100 pps stimulus is lower than that for the 400 pps stimulus.. For the 100 pps data, more than a vertical shift is required to align

the threshold curves in figure N. There appears to be a significant interaction between pulse width and pulse rate at 100 pps. Of the stimulus set measured, the 100 pps stimulus exhibits the « narrowest » or smallest dynamic range at the small pulse widths, but the largest dynamic range at the large pulse widths.

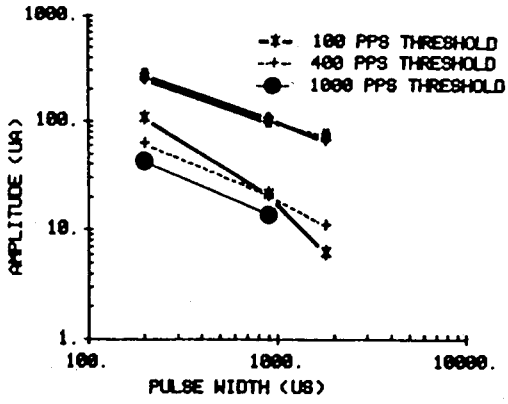

Fig. 24. - Threshold and MCL as a function of pulse width at 100, 400, 1000 PPS and a burst duration of 300 msec. Data is from subject B with bipolar electrode pair (7, 8) stimulated.

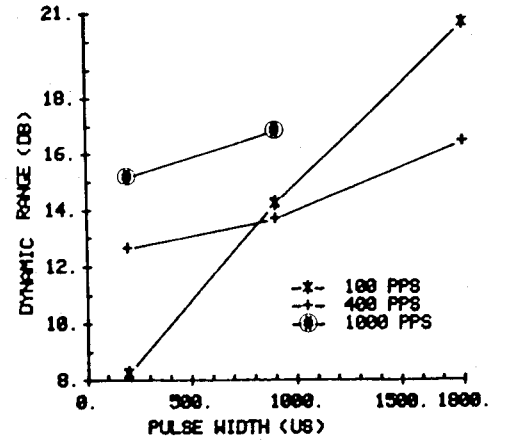

Fig. 25. - Dynamic range as a function of pulse width at 100, 400, 1000 PPS and a burst duration of 300 msec. Data is from subject B with bipolar electrode pair (7, 8) stimulated.

Temporal integration of two-channel stimuli

The previously described results indicate that some form of short-term temporal integration may be present in subjects A and B. This section presents evidence for one type of short-term temporal integration process: « temporal integration at the nerve membrane ». One peripheral nerve mechanism that might produce temporal integration was described by Butikopfer and Lawrence (1979) and was briefly reviewed in section 4.

When the current generated by two or more stimulus pulses enters the nerve membrane, some of the « residual » or « remaining » excitation due to the first pulse may reduce the nerve's threshold such that the second pulse may elicit an action potential, even though the second pulse alone, could not have elicited an action potential (Butikopfer and Lawrence, 1979). The location of the generator's of these two current pulses is not significant in this model. Only the stimulus magnitude of the current reaching the nerve and the relative timing of these pulses is significant. In fact, the two stimulus pulses could originate from entirely different location as long as sufficient current from both electrodes was developed at the point of excitation and as long as the pulses were temporally « close to each other ».

Figure 26 illustrates the loudness estimates that subject A made when the two biphasic pulses came from separate electrode channels plotted as a function of the delay between the two pulses. Loudness increases significantly when the inter-pulse delay (or duration) is reduced below 5 msec.

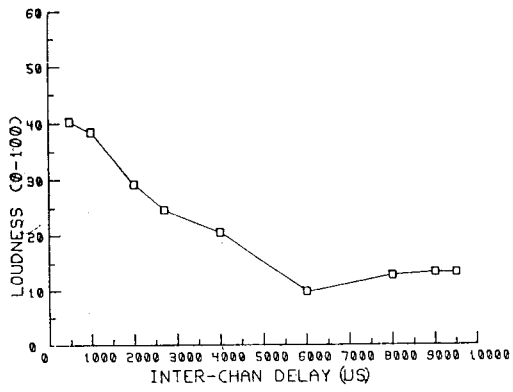

Fig. 26. - Loudness as a function of the delay between the initiation of single 200 µsec biphasic pulses on two channels. The first channel was monopolar electrode (1) and the second channel was monopolar electrode (7). Subject A made 9 loudness estimates for each of the interchannel delays.

Two factors are necessary to cause a change in the subject's loudness estimates when stimulating two electrode channels with fixed amplitude and fixed pulse-width biphasic pulses. First, *each* of two electrode channels must produce a significant current density at one or more *common* nerve membrane locations. Second, the delay between pulses should be below 1-2 msec to elicit the loudest percepts; and the delay between pulses should be greater than 4 to 5 msec to elicit the lowest loudness estimates. We would expect to observe an increase in loudness when we change the interpulse delay from 5 msec to 1 msec, *if* there were enough fibers that received a significant amount of current from both of the two channels. In contrast, if none of the fibers received a significant amount of current from *both* electrode channels, we would not expect to observe a significant change in loudness as the inter-pulse delay was changed from 5 msec to 1 msec.

A set of experiments were conducted in which the loudness was measured as a function of three variables: the inter-pulse delay, the distance between electrode channels, and the electrode channel geometry. Two subjects were tested in this series of experiments. The electrodes were either monopolar or bipolar (with contacts oriented radially and an intercontact separation of approximately .7 mm). As the distance between electrode channels was increased, the *change* in loudness (due to the change in inter-pulse delay) decreased very significantly. The type of electrode was a very significant factor in the loudness function. Bipolar electrodes as compared to monopolar electrode channels significantly reduced the extent of these two-channel interactions.

Figure 27 illustrates how two monopolar channels interact when the stimuli from the two channels are not temporally overlapping. The subject was asked to adjust a slide pot in accordance with how loud the stimulus was. The slide pot was graduated on a scale of 0 to 100; where « 0 » was just below threshold and « 100 » represented the maximum comfortable loudness (MCL).

Loudness estimates were obtained for a pseudo-randomized set of stimuli in which the delay between the pulses on the two channels was varied. Inter-channel delays were set to one of eight values. Delays of .5, 1, 2, 4, 6, 8, 9, 9.5 msec were used. The interaction was measured as a function of interchannel delay and distance between the two channels. Instead of using one pulse per channel, each channel was stimulated at a rate of 100 pulses per second. This experimental modification i.e., lengthening the burst duration) made the task simpler for the subject, but does not change the basic interpretation of the experiment. Each biphasic pulse was 200 µsec (100

μsec/phase) in duration. The pulse train was presented for 300 msec.

In figure 27, monopolar electrodes were used for both chanenls. Each curve illustrates the interaction between two monopolar channels at a different inter-channel separation. The curves are ordered such that the interchannel separation increases in 2 mm steps, from a starting separation of 2 mm (in the top curve), to an interchannel separation of 14 mm (in the bottom curve). As the distance between the two electrodes was increased, the amount of interaction decreased. In this subject (A), interaction

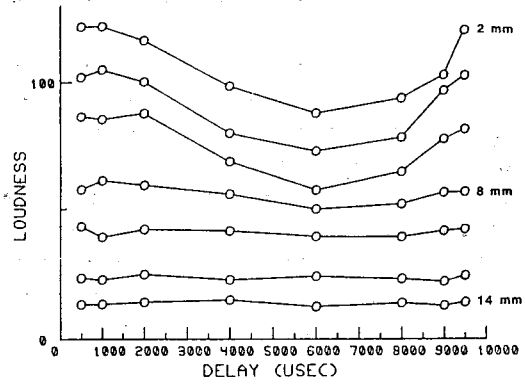

Fig. 27. - Subject A's loudness estimates as a function of the delay between pulse trains on two monopolar electrodes and as a function of the distance between the two electrodes. The loudness estimates have been shifted vertically on the loudness scale (0-100) for readibility. One of the two stimulated electrodes was the most apical monopolar electrode (ie electrode « 1 »). The other stimulated channel was a monopolar electrode located either 2, 4, 6, 8, 10, 12, or 14 mm from electrode (1). Each of the two channels was driven by a 100 pps, 300 msec, biphasic pulse train with pulse widths of 200 μsec (100 μsec/phase). In the top four curves, twelve loudness estimates were obtained for each of the eight interchannel delays. The subject made only four to nine loudness estimates for each inchannel delay in the last four curves.

between monopolar electrodes was quite significant at a distance of 6 mm. Interaction decreased at an 8 mm interchannel separation and was negligible at a 10 mm interchannel separation. The difference between the mean loudness for a 1 msec interchannel delay and the mean loudness for a 5 msec interchannel delay. The difference in loudness was divided by the average of the two means and then multipled by 100 to obtain the « percentage change in loudness ». This index is a measure of the interaction between two channels and will be referred to as an « interaction index ».

$$\text{Index} = 100 * (\text{Lmax} - \text{Lmin}) / [(\text{Lmax} + \text{Lmin})/2].$$

Figure 28 summarizes data obtained from subjects A and B. The interaction index is plotted as a function of inter-channel distance and electrode geometry (bipolar or monopolar). The two subjects are dramatically different in this function, with subject B exhibiting considerably less interaction than subject A. As previously stated, channel interaction « drops off » with inter-channel separation and is further reduced with bipolar stimulation. When bipolar electrodes were stimulated in subject B no statistically significant changes in loudness were detected at even the smallest interchannel separation of 2 mm.

At the same interchannel separation, loudness changes significantly more (as the interchannel delay is varied) with monopolar stimulation than with bipolar stimulation.

Interestingly, the fact that the electrode configuration has a strong effect on such « channel interactions » supports the concept that these temporal interactions are occurring at a peripheral rather than a central location. (1) When stimulated alone, each channel (whether monopolar or bipolar)

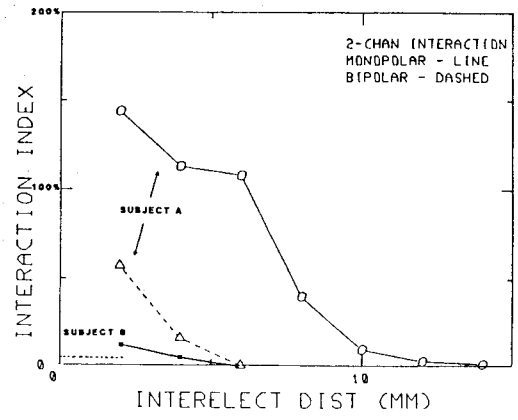

Fig. 28. - Temporal interaction as a function of interchannel distance, electrode geometry, and subject (A or B). The two subjects are dramatically different in this measure, with subject B exhibiting much less interaction than subject A. Monopolar electrodes are represented with solid lines. Subject A's bipolar electrodes are represented with a dashed line. There was no measureable interaction with bipolar stimulation of even adjacent channels in subject B. The distance between the horizontal dashed line and the horizontal axis represents the standard error of the interaction index for subject B with two channel bipolar stimulation. In both subjects, the same monopolar electrode configurations were used at each interchannel separation (see legend of figure 27). The bipolar electrodes were located at the same « cochlear place » as the monopolar electrodes. For example, bipolar electrode (1, 2) is approximately « located » in the same position as monopolar electrode (1).

elicited approximately the same loudness. (2) For the same interchannel separation, monopolar and bipolar electrodes were at nearly the same cochlear locations. Under these circumstances, we might assume that any given monopolar electrode would excite nearly the same population of fibers that « its » bipolar equivalent (i.e., same location — same loudness) would excite. This, of course, is not certain but is quite plausible. Let us assume for the moment that the changes in loudness were due to central mechanisms sensitive to the delay between the two channels. If this and the previous assumptions were correct, the monopolar and bipolar electrode configurations should generate nearly identical loudness changes for any given change in interchannel delay. However, monopolar and bipolar configurations *do not* generate similar changes in loudness for a given change in « interchannel delay ». If (1) and (2) are « sufficiently accurate », then it is likely that the source of the temporal interaction is peripheral. The peripheral-nerve, temporal integration process discussed in section 4 may be a likely candidate. In these two channel experiments, each of the monopolar electrode channels probably excite approximately the same number of fibers as their bipolar counterparts, but it is likely that a greater number of fibers are « just below » threshold after the first monopolar channel's stimulus pulse than in the bipolar case. This is likely the situation, because monopolar electrodes generate a greater current spread.

Discussion

Behavioral threshold is a function of pulse rate, pulse width, and burst duration. Relatively simple phenomenological models of threshold behavior can be useful in describing many characteristics of threshold behavior. This section considers how these models can relatively accurately summarize the experimental data. Many of these simple phenomenological models directly suggest one or more alternative mechanisms.

THE THRESHOLD FUNCTION

The threshold function will be described in two parts. Thresholds to single pulses and cycles will be considered first and then extended to thresholds of multiple pulses and cycles.

THRESHOLDS TO SINGLE PULSES AND SINGLE SINE WAVE CYCLES

Threshold functions for single biphasic pulses and single cycle sine waves are similar. Hill's model only roughly approximates the behavioral threshold function for single cycle sine waves and single pulses (Figs. 9 and 7). In a « best-fit » Hill's model, threshold increases above 50-100 Hz to 6 dB/octave. Behavioral threshold to single cycles deviates from this model in two frequency regions. Threshold does not increase quite as much as 6 dB/octave (perhaps an average of 5 dB/octave over the 1000-4000 Hz range) at the higher frequencies (or at the shorter pulse widths). This data indicates that shorter cycles and pulses require slightly less charge for excitation. McNeal (McNeal, 1976; McNeal, 1977) has shown that the shorter pulses are more effective in exciting the nerve than would be predicted from Hill's « constant-charge » model. Hill's model is most directly applicable to electrical stimulation of an excitable membrane in which one electrode is intra-axonal and the second electrode is located across the membrane in the extracellular medium. McNeal developed a more realistic electrical stimulation model of myleneated nerve by assuming that both electrodes are extracellular and at specified locations relative to the nodes of Ranvier.

In Hill's model, *all* current that is generated at the electrodes must traverse the membrane and therefore all the generated current contributes to the excitation of the nerve membrane. In McNeal's model, the current generated at the electrodes is not constrained to enter the nerve fiber. Some percentage of the current may never enter the nerve fiber and therefore not contribute to excitation. Part of the current generated at the electrodes, may simply be shunted around the nerve by the surrounding ionic medium. The relative amount of current that passes through the nerve membrane depends on the relative impedance of the nerve pathway (composed of the membrane and inter-axonal impedances) compared to the impedances of the alternative current paths. Here we assume that the surrounding medium can be approximately modelled by a pure resistance (Spellman, 1982). A greater percentage of the *total* stimulus charge will flow into the nerve when the pulses are shorter; because a greater proportion of stimulus charge flows through the membrane capacitance during the earlier portions of the stimulus pulse. In other words, the membrane capacitance offers a lower impedance to the higher frequency stimulus components. Therefore, threshold current does not increase at a 6 dB/octave rate, but at a somewhat lower rate, because shorter pulses (cycles) require less charge to excite the nerve.

This « frequency response » function is likely a second-order function of the distance between the neural process and the stimulating electrode(s) as well as the electrode configuration.

As pulse width is increased above 1 msec, hyperpolarization generated by one phase of the stimulus may increase the nerve's sensitivity to the following phase of depolarization. As a conseguence, the thre-

shold may decrease at a greater rate than 6 dB/oct as the cycle duration is increased above 1 msec. Typically, the average slope between 1000 and 100 Hz is 9 dB/octave for *single* cycles and *single* pulses. Such a mechanism has been described in section 3.

A slightly more complex linear filter than that in Hill's model would more accurately model threshold behavior for single cycle sine waves and single pulse stimuli. The filter would have a slope of approximately 4-6 dB/octave for frequencies above 1000 Hz and 9 db/octave for frequencies below 1000 Hz. The frequency response would « flatten-out » for frequencies below 100 Hz. Data for cycle durations longer than 20 msec (or equivalently, 50 Hz) were not obtained because maximum charge density limits would often have been exceeded.

In summary, the nerve's threshold for single cycles or single pulse varies at roughly 6 dB/octave for cycle duration less than 10-20 msec. However, significant second order effects alter the threshold function over certain frequency-pulse-width regions. For single pulses or cycles shorter than about 1000 μsec, threshold increases at a rate somewhat less than 6 dB/octave. For single biphasic pulses or single sinewave cycles longer than 1000 μsec and shorter than 10-20 msec, threshold increases at a higher rate than 6 dB/octave (about 9 dB/octave) as the stimulus frequency is increased.

Multiple pulse and cycle thresholds: the higher pulse rates

By using single sinusoidal cycles or single biphasic pulses, a first-order estimate of the system's frequency response can be obtained with little « contamination » in this frequency response measure due to central or peripheral temporal integration of excitation generated by multiple pulses or cycles.

In this section we compare the thresholds obtained with multiple cycle stimuli to those thresholds obtained with single cycle stimuli. Since the stimulus spectrum (when measured with a time window of approximately the same shape and duration as the impulse response of the linear filter within Hill's « best-fit » model) is affected ~~not~~ only to a second order by changing the burst duration or the pulse rate, the difference between single-cycle and multicycle thresholds can be used as an estimate of the significance of, and the time order of, any temporal integration process(es). Exceptions to this generality will be noted later in the text.

Threshold is a strong function of both pulse rate and burst duration. Threshold effects that can be reasonably approximated with only a simple linear filter model were discussed in the previous section dealing with single sine cycles and pulses. To include the effects of multiple pulses (i.e., the effects of pulse rate and burst duration), an addition to this filter model is required. When the stimulus contains more than one biphasic, charge-balanced cycle the linear filter model for threshold behavior should be extended to include temporal integration.

Temporal integration mechanisms appear to be useful in describing threshold behaviour to stimuli with multiple pulses. A description of several of the most probable temporal integration mechanisms presented at the end of this section. The following response characteristics are well modelled by temporal integration processes:

1) The threshold decreases as the number of pulses increase (see figure 11). Correspondingly, threshold decreases as the burst duration increases (see figures 18, 19

and 20). In general, threshold decreases as burst duration is increased for burst durations as long as 80-160 msec. This suggests that at least one of the temporal integration mechanisms contains a relatively long integration window.

2) In figure 12, threshold decreases as the temporal spacing between the pulses decrease. The decrease in threshold as the interpulse interval is decreased is particularly significant for pulse trains with interpulse durations less than some critical value. This critical value may be a useful measure of at least one of the « time windows » of integration. In figure 12, when the interpulse interval drops below 5 msec, threshold decreases at a considerably greater rate for equal increases in the burst duration. Similarly, in figures 13 and 14, threshold drops at a much greater rate for pulse rates above 200 pps (i.e., the interpulse interval is less than 1/200 pps = 5 msec).

3) For sinusoidal stimuli above 400 Hz, thresholds for 300 msec bursts are lower than those of single cycles (see figure 9). The deviation between the single cycle threshold curve and the 300 msec threshold curve increases as the frequency is increased above 200 Hz. Thresholds for long-duration, higher frequency stimuli are considerably lower than thresholds for single cycles of the same frequency, probably because more stimulus cycles occur within the integrating time window of the hypothetical temporal integrator(s).

4) Loudness changes as a function of the delay between pulsed on two nearby channels (see figures 26 and 27).. Because the extent and amount of this interaction is highly dependent on the electrode configuration (e.g., monopolar vs bipolar), this data lends support to the peripheral origin of at least one of the temporal integration processes (see Section 9). Since this two channel temporal interaction occurs primarily over a 2-5 msec time window, this data supports the peripheral origin of a short-term temporal integration mechanism with an integration window of approximately 2-5 msec.

Partial integration of subthresohld depolarization at the nerve membrane (see section 4) is one process that could generate response features similar to some of those features described above (i.e., those features asosciated with relatively short integration intervals). This mechanism is particularly attractive in describing, at least, the shorter term temporal integration properties which appear in the threshold behavior. A longer term integrative mechanism also appears to be active. At very low pulse rates and at relatively long burst durations, threshold decreases as the burst duration is increased (e.g. figures 18, 19 and 20). This behavior may be the result of a longer term integration process. Such an integrative mechanism could be the result of a central neural temporal integration mechanism *or* a peripheral-nerve-process temporal integration mechanism. Certainly, a central integration mechanism has appeal because of the strong evidence for its existence in the normal auditory system. Some of the possible mechanisms for temporal integration are described in the next section.

Possible temporal integration mechanisms

Threshold changes very significantly with the duration of the stimulus for both pulse trains and sinusoidal bursts. At least some combination of three mechanisms may be involved:

(1) For the higher stimulus frequencies, peripheral nerve temporal summation

may cause the threshold to decrease as the duration of the stimulus is increased. This mechanism was described in the introduction. This effect is particularly apparent for the 1000 pps pulse train thresholds displayed in figures 18 and 19. This effect is also illustrated in figure 11 where threshold decreases significantly as the number of pulses is increased. In general, threshold drops, as duration is increased, and most significantly for monopolar electrodes, and for those bipolar electrodes with wider pair spacing. In figure 19, the 1000 pps monopolar threshold drops significantly more than does the bipolar (figure 18) threshold for 1000 pps as the train duration is increased from approximately 1 msec to 20 msec. Figure 9 displays thresholds to 300 msec sinusoidal bursts and single cycles. Above 200 Hz, the threshold decreases significantly as the duration is increased. For these higher frequencies, peripheral nerve temporal integration may be at least one of the reasons for significant drops in threshold.

(2) Central temporal summation. If spontaneous activity is generated peripheral to the hypothetical « neural detection center », detection of a stimulus may require more than simply detecting the presence or absence of neural activity. Some form of temporal integration would likely be necessary. If the neural input contains both noise and signal, then an ideal detector will exhibit lower thresholds for longer burst durations (Green and Swet, 1964). As a consequence, such central temporal summation may be responsible for some of the drop in threshold as the burst duration is increased.

(3) Stochastic nature of the nerve's excitability. The nerve's threshold is not constant. The nerve's threshold varies over time (Verveen, 1959). The addition of noise to a deterministic model of neural threshold should form a more accurate neural threshold model (White, 1983). In such a model, the probability of excitation is increased as the burst duration is increased. In a first order model of this behavior, each stimulus cycle could be conisdered an independent trial. As the burst duration is increased, the number of trials increases proportionately. The probability of at least one or « N » firing(s) increases as a consequence of the increased number of « trials ». From (1) above, there is evidence that each trial is not necessarily independent of the previous trials. Indeed, previous stimulus cycles may tend to increase the probability of firing to subsequent stimulus cycles.

13. Multiple pulse and cycle thresholds: the lower pulse rates

Up to this point, we have primarily considered responses to stimuli with pulse rates between 400 pps and 4000 pps and sinusoidal stimuli with frequencies between 400 Hz and 4 kHz. For stimuli with pulse rates between 50 pps and 200 pps a rather more complex pattern of behavior exists.

Threshold responses are quite dependent on both stimulus' pulse width and pulse rate. These two factors significantly « interact ». For pulse widths shorter than 500 to 1000 μsec, responses are similar to what would be predicted from the 2-integrator model useful in describing threshold behavior for the higher pulse rate stimuli. Because the pulse rates discussed here are relatively small (i.e., 50-200 pps), the hypothetical short-term integrator will only play a minor role with such low-pulse-rate stimuli. The effects of the hypothetical longer-term (integration windows on the order of 80-160 msec) temporal integrator are best illustrated in figures 18 and 19 for the 100 pps and 200 pps, 200 μsec pulse width

stimuli. Only small decreases in threshold (2-4 dB) occur for quite large increase in burst duration (from 200 μsec to 100 msec).

A threshold model for single pulses needs to be an integral part of such a multi-pulse model. The single pulse model is probably best placed just prior to the « slow » integrating process in this multi-pulse model.

Thus, for short pulse width, low repetition rate stimuli the previously described model for high-pulse rates should be quite useful. However, if the pulse width is greater than 500-1000 μmsec, the complex behavior of neural excitation becomes considerably more apparent. Single pulse behavior for large pulse widths has been discussed in section 11. At least two mechanisms may be involved in reducing thresholds for these single, longer-duration pulses:

(1) The quantity of charge entering the neuron increases with the pulse width. This would cause only a .6 dB/octave change in threshold if a simple resistor-capacitor and voltage detector membrane model is used.

(2) The nerve may become more sensitive to the depolarizing phase of the stimulus after being driven by the hyperpolarizing stimulus phase (see section 3).

With multiple, long-duration pulses, threshold decreases most significantly for pulse rates near 100 pps and sinusoidal frequencies near 100 Hz (see the 1800 μsec pulse width threshold curve in figure 23). In figure 9, threshold is significantly lower for multiple 100 Hz cycles than for single 100 Hz cycles. The difference in thresholds for multiple cycles vs single cycles is considerably less for the « surrounding » 50 Hz and 200 Hz frequencies.

Perhaps most interesting is the data displayed in figure 24. Here we examine threshold and MCL as functions of pulse width and pulse rate. The 100 pps threshold curve deviates significantly from the pattern of the 400 pps and 1000 pps threshold curves, particularly for pulse width greater than 1000 μmsec. Most remarkable is the clear evidence for a lower threshold at an 1800 μsec pulse width for the 100 pps, as compared to the 400 pps threshold. This is remarkable because the 400 pps, .3 sec stimulus, contains four times as many 1800 μsec pulses as does the 100 pps stimulus! Furthermore, the 400 pps stimulus has much more closely spaced (i.e., temporally) pulses than does the 100 pps stimulus. It appears that longer pulses augment the sensitivity of the system to subsequent pulses if the interpulse interval is near 10 msec. If the interpulse interval is closer to 20 msec or 5 msec, prior pulses or cycles do not generate such significant increases in the system's sensitivity (see figure 9). Such behavior is not that which would be generated by some form of temporal integration. In particular, the system's sensitivity is greater for 1800 μsec pulses temporally spaced 10 msec apart than for 1800 μsec pulses spaced 5 msec or 2.5 msec apart (Fig. 24). A temporal integrator should exhibit at the minimum, the same sensitivity (and generally more sensitivity) to more closely spaced pulses.

Figure 29 illustrates the significant drop in threshold for a 100 Hz sinusoidal stimulus as the burst duration is increased. For short (200 μsec) biphasic pulses with a 100 pps repetition rates, behavioral threshold does not drop nearly as significantly as does threshold for 100 Hz sinusoidal stimulus (see figure 29). The longer duration of each phase of the 100 Hz sinusoidal stimuli may be necessary for the process which reduces the threshold to this type of stimulus.

Perhaps in an analogous manner, each stimulus cycle appears to increase the pro-

bability of an AVCN cell's firing during the initial 20 to 40 msec of 100 Hz stimulus (see figure 30). This has been a very consistent feature of presumptive AVCN large spherical cell responses to 100 Hz sinusoidal stimuli. Such slow response onsets were nearly non-existent for 200 Hz and higher frequency sinewaves.

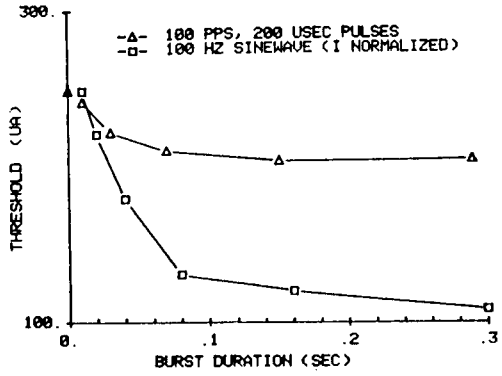

Fig. 29. - Threshold stimulus current as a function of burst duration for two types of stimuli: a 100 Hz sinusoidal burst and a 100 pps train of 200 usec biphasic pulses. Data is from subject A with electrode pair (1, 2) stimulated. The 100 Hz threshold currents have been shifted vertically (by multiplying each 100 Hz threshold value by a factor of 13.3) on the log scale to obtain a better visual comparison.

White, Merzenich and Loeb (& Whit) have discussed a set of alternative mechanisms for this slow-onset behavior: The Frankenhaeuser-Huxley model describes many of the effects of the more quickly acting nerve membrane phenomenon. It is not clear whether the F-H model can accurately predict such long-term effects as those described in the previous paragraph. A slower feature of nerve excitation (which is not incorporated in the F-H model) may play a role in the slow « build-up » of firing. During electrical stimulation, extracellular ionic concentrations (e.g. the Potassium concentration) could change enough to alter the excitability of nearby neurons (Moran and Palit, 1980). This effect can occur over a time interval of tens of milliseconds. During excitation or subthreshold stimulation, sufficient quantities of one or more ions could flow into the extracellular medium and therefore affect fiber excitability.

It is also possible that the build-up effect may be due to neural processing in the brainstem with excitatory feedback pathways onto AVCN neurons. If his were the case, the described slow onset of responses to 100 Hz sinewave bursts would presumably not be present in eighth nerve responses to this type of electrical stimulus.

The MCL Function

For subjects A and B, MCL decreases only slightly as the pulse rate is increased (see figures 13 and 23). For these subjects (A and B), maximum comfortable loudness is not a strong function of burst duration (see figures 16 and 9). MCL is only a very weak function of pulse rate. Pulse width, on the other hand, has a considerably stronger influence on MCL than does either pulse rate or burst duration. MCL decreases at about 3-4 dB/per octave of pulse width (e.g. see figures 7 and 24). Likewise, for sinusoidal stimuli with frequencies above 200 Hz, MCL increases at about 3-4.5 dB/octave (e.g. figure 9). MCL behaves similarly for both pulse and sinusoidal stimuli as a function of the duration of the cycle.

MCL varies significantly with the signal's spectrum; but MCL varies relatively little with burst duration or pulse rate. Because MCL is only weakly influenced by

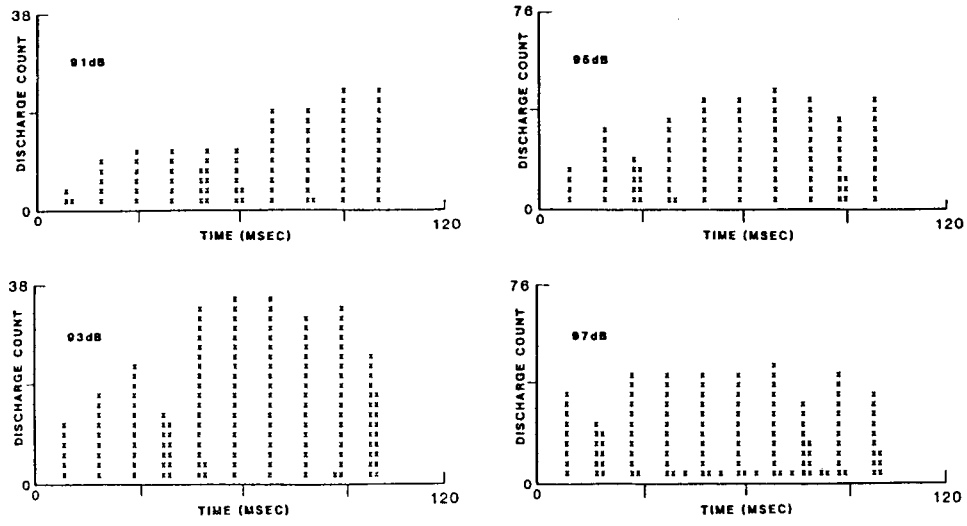

Fig. 30. - Post stimulus time histogram series wich illustrates the gradual onset of a presumably large-spherical AVCN cell's response to an electrical stimulus of 100 Hz. As stimulus level is increased, the response « rise-time » is considerably shortened in these single unit recordings in cat. Note that the vertical scale changes from 38 spikes maximum to 76 spikes maximum in the two histograms representing responses to the two highest stimulus levels. Illustration from White, Merzenich, and Loeb, 1983.

burst duration or pulse rate, there is evidence for only a relatively small amount of temporal integration *at the periphery* at these high suprathreshold stimulus levels. However, a considerable amount of *central* temporal integration may exist. If only a small increase in the stimulus level is necessary to excite a large number of additional fibers, only small increases in MCL would be necessary to generate a sufficient quantity of « neural activity » which would totally compensate for the neural activity that was « lost » because of a decrease in burst duration and/or pulse rate. This explanation uses a simple « total-neural-activity » model for central temporal summation (see section 18).

To a first approximation, the MCL function could be modelled by a simple linear filter with a frequency response function of approximately 3-4.5 dB per octave over the frequency range of 100-4000 Hz; MCL increasing with frequency. From 50-100 Hz, the filter's slope is approximately zero (i.e., there is little or no change in MCL). In this simple model, a « threshold detector » is placed after the filter. When the voltage across the detector reaches a specified value, the maximum comfortable level is « signaled » or « elicited » in this model.

A temporal integrator is not included in this first order model because MCL is only a weak function of pulse rate and burst duration. In contrast to the threshold function, MCL is only a weak function of those stimulus variables (i.e., pulse rate, and burst duration) which would cause significant

changes in MCL if a *peripheral* temporal integrator was present. As previously discussed, a central temporal integrator would not necessarily cause even moderate changes in MCL as burst duration or pulse rate are changed; particularly if small changes in stimulus amplitude recruit relatively large numbers of fibers.

A filter model of the MCL function is only a first-order approximation. For example, burst duration has a small but noticeable affect on the shape of the MCL vs frequency curves in figure 9. At the higher frequencies, the single cycle MCL function increases at a slightly greater rate than does the MCL function to the 300 msec stimuli. This small effect cannot be simulated by the proposed linear filter model alone. The small amount of temporal integration that is exhibited in the MCL function is of a considerably smaller magnitude than that exhibited in threshold functions. There are at least three possible explanations; any combination of which may be responsible: (1) Those fibers that are excited at, and near, threshold levels may exhibit a very significant amount of temporal integration; however, the presumably many additional fibers that are excited at MCL levels may exhibit little or no temporal integration (or may have a much shorter time window of integration). This will be refered to as the « two-population model » and is discussed further in section 17. If we assume that loudness and therefore MCL is a function of total neural activity (see section 18), then the MCL function would reflect properties of both neural populations. Therefore, we would expect some influence, although reduced, from the temporal integration associated with those fibers excited near threshold levels.

(2) A central temporal integration mechanism may be at least partially responsible for the auditory systems added sensitivity to multiple cycles at the higher suprathreshold (as well as at threshold levels). If small increments in stimulus amplitude (at MCL levels) cause relatively large increases in the number of excited nerves in a given subject, only a *small* increase in the stimulus level would be necessary to maintain identical amounts of total neural activity even if the burst duration was quite significantly decreased.

(3) For that portion of temporal integration that is due to a central temporal integration mechanism, another or additional factor may be at least partially responsible for the relatively small changes that are required in stimulus level at MCL for very large changes in burst duration. Both eighth nerve (& Moxon) and AVCN (& White) responses to suprathreshold electrical stimulation of the auditory nerve exhibit significant amounts of adaption. Specifically, responses to stimuli significantly above neural threshold respond at a higher firing rate during the initial 5-20 msec segment of the stimulus (estimate of time course). If this is also the case with implanted subjects, total « summed » neural activity would not be proportional to the duration of the stimulus. For example, of a relatively long duration stimulus (say 20-40 msec) is doubled in duration to 40-80 msec, the total neural activity would be significantly less than double that for the 20-40 msec stimulus simply because *both* stimuli elicited a relatively large portion of total neural activity during the first interval of the response.

Summary of the threshold and MCL fuctions

This section reviews both threshold and MCL behavior and suggests model that may be useful in the interpretation of « mid-range » functions such as loudness and intensity discrimination. In one sense, threshold and MCL functions are simply the two extremes of an infinite set of equi-loudness functions. By understanding what differences exist in threshold and MCL behavior, we should be able to synthesize « integrated » models which describe both threshold and MCL behavior. At least three response features are distinctly different for threshold vs MCL functions. The following discussion considers these differences and describes alternative interpretations.

The MCL function can be approximately represented as a linear filter followed by a non-integrating threshold detector. For single cycles, the filter's frequency response is approximately 3-4 dB/octave above 100 Hz (see figure E). At longer burst durations, the MCL function deviates slightly from a constant slope of 3-4 dB/octave. This deviation is probably not due to the small spectral difference in the two stimuli, since the small spectral change would cause a change of excitation in the opposite direction to that observed. Because the shape of the MCL functions frequency response is different, although only slightly, for the two different stimulus durations, the simple filter model can only be an approximation to the MCL function. Temporal integration process(es) may cause the MCL function to deviate from the linear filter function as the number of cycles is increased. In figure 9, at frequencies above 200 Hz, the shape of the two MCL curves differ from each other in a qualitatively similar manner to how the two threshold curves differ from each other. This could indicate that the essential mechanism responsible for the difference in the two MCL curves is identical to that responsible for the two threshold curves. Both pairs of curves diverge as the frequency is increased above 200-400 Hz. This behaviour is consistent with that behaviour which would be generated by the previously discussed peripheral nerve temporal integration mechanism.

Short-term temporal integration: threshold and MCL functions

In two subjects (A and B), threshold responses demonstrated behaviour consistent with a very significant component of short-term temporal integration. In contrast, the MCL functions were only slightly affected by this presumed short-term temporal integration process. In the third subject (C), neither the threshold nor MCL funtions behaved in a manner consistent with that typically associated with a short-term temporal integration process.

Two population model

One model that would integrate the short-term temporal integration properties of both the threshold and MCL models would incorporate two or more functional neural populations. In this model we do not need to assume that two or more distinct types of fibers exist, only that two or more types of peripheral neural responses can exist to identical electrical stimuli. Different types of responses could originate from the same neuron, if the initial site of excitation (ISE) was different. In this model, one of the neural populations (group A) would exhibit a significant amount of « pe-

ripheral-nerve, temporal-integration; the other population (group B) would exhibit little or no « peripheral temporal integration » or would exhibit a considerably shorter temporal integration time window. In this model, we assume that loudness, and therefore MCL, is monotonically related to the overall amount of neural activity contributed by both populations. We will assume that group A responses exhibit the lowest thresholds (because the fibers are presumably closer to the stimualting electrodes and/or because the processes or ISE's are exceptionally sensitive). As a consequence, threshold functions would strongly exhibit behaviour representative of a temporal integration process. In contrast, MCL functions may only exhibit a relatively small amount of temporal integration, since only a fraction of the total number of excited fibers would « temporally integrate » the stimulus.

Herndon (1981) found two groups of behavioral responses depending on which of four modiolar electrodes were stimulated. Specifically, Herndon discovered that thresholds to biphasic pulse stimuli decreased very significantly as a function of pulse rate for two monopolar electrodes, and did not decrease noticeably for the other two monopolar, modiolar electrodes (fig. 31). In his study, the stimulating electrode array was located in the modiolus and therefore might be expected to sample a different, and perhaps larger distribution of nerve processes than would be sampled by a scala tympani electrode array. Interestingly, Herndon (1981) reports that thresholds were constant with pulse rate for *all four* electrodes *if* quite short, exponentially-shaped biphasic stimulus pulses were used (see figure 32). This would indicate that only an amplitude and time-dependent non-linearity (e.g., the

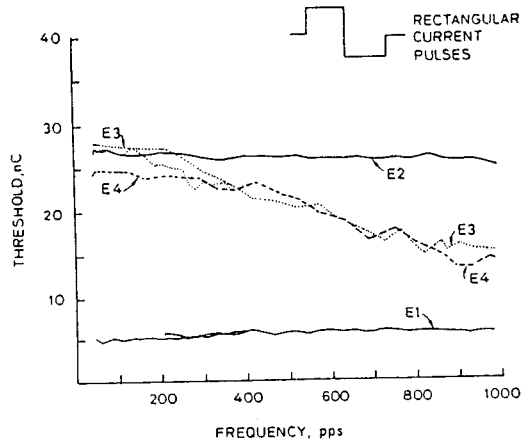

Fig. 31. - Threshold as a function of pulse rate for biphasic current pulses. These threshold functions were obtained by Herndon (1981) using an electrode array implanted in the modiolus. Pulse widths were 200 μsec. Figure courtesy of Matt Herndon.

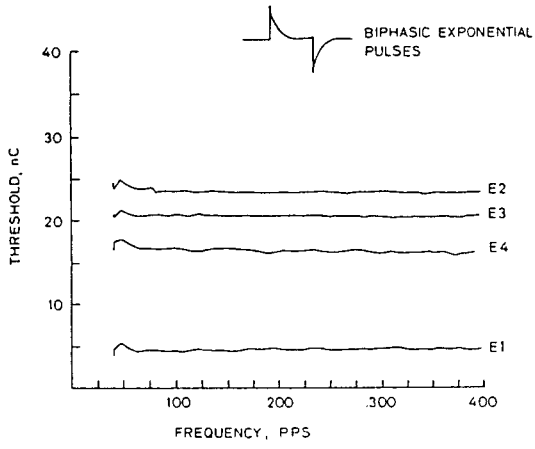

Fig. 32. - Threshold as a function of pulse rate for very short-duration « biphasic-exponential » pulses. The majority of charge transfer occurs in less than 25-50 μsec per phase. These threshold functions were obtained by Herndon (1981) using an electrode array implanted in the modiolus. Figure courtesy of Matt Herndon.

H-H or F-H model) could accurately model this behavior.

Van Den Honert (personal communications) in single neuron recordings in eighth nerve has found evidence for two types of neural responses to electrical stimulation. At low stimulus, a longer latency response is elicited. This response exhibits distinctly different refractory behavior than that observed for the shorter latency responses generated at the higher stimulus levels. They have been able to eliminate the longer latency response component by destroying eighth nerve ganglion cells and dendrites, but leaving the axons intact. They believe that this behavior is due to two distinct sites of excitation. One site (with its own response characteristics) may be excited at lower stimulus levels and another site is excited at the higher stimulus levels.

With scala tympani stimulation, one type of threshold behavior has been observed in subjects A and B. These subjects have demonstrated threshold functions consistent with a peripheral, short-term integration process. Very recently, a third subject (C) has been tested psychophysically and does *not* exhibit behavior consistent with the presence of this peripheral, short-term temporal integration process. This subject is completely devoid of two-channel temporal interactions (see section 9) at inter-channel delays greater than .5 msec and does not display significant decreases in threshold as the inter-pulse interval is decreased from 5 msec to 1 msec if the number of pulses is held constant. Observations during surgery, the subject's etiology, psychophysical field interactions measures, and ABR threshold and magnitude measures indicate that this subject probably has a very low nerve survival. It is possible that this recent subject (C) is nearly or totally devoid of group A processes and therefore does not exhibit the specific set of response features associated with this type of peripheral, short-term integration porcess.

With all three subjects, there is significant evidence for another temporal integration process which exhibits a considerably longer duration integration window (approximately 80-160 msec). It appears that the longer-term temporal integration mechanism may be distinct and separate from the hypothetical shorter-term temporal integrator, simply because only two of the three subjects exhibited both forms of temporal integration.

Another model that could account for differences between these threshold and MCL responses could be proposed. This model is very similar to that proposed in the next section (section 18) to account for certain features representative of long-term (80-160 msec) temporal integration. In this model a central integration process is proposed. It is proposed that threshold and MCL functions of burst duration and pulse rate are different because the « recruitment » of excited fibers is a non-linear function of stimulus intensity. It is proposed that MCL functions may be more shallow than threshold funtcions of burst duration and pulse rate in subjects A and B because many more additional fibers are excited for a given increase in stimulus intensity at MCL levels than at threshold levels.

However, this model is only useful in describing behavior associated with a *central* temporal integration mechanism that sums *already-generated* neural activity from numbers of fibers. Contrary to that model's assumptions, the evidence presented in sections 9 and 4 indicates that the *short-term* temporal integration mechanism originates prior to, or at the point of excitation along

the peripheral neural process. Spellman's data (1982) indicates that only linear processes occur within the tissue surrounding the nerve processes; and therefore it is highly likely that the short term temporal integration process occurs at the highly non-linear nerve membrane during the process of neural excitation.

Long-term temporal integration: threshold and MCL function

With all three subjects (A, B and C), there is strong evidence for a second temporal integration mechanism which has a considerably longer integration window. For example, in figures 18, 19 and 20, all threshold fucntions decrease with increasing burst duration for burst durations as large as 80-160 msec. MCL functions also decrease with burst duration, even for burst durations as large as 80-160 msec. However, in general, the change in MCL (in dB) for a given change in burst duration is not as great as that seen in the threshold functions. For example, in figure 14, MCL changes only slightly compared to changes in threshold when the burst duration is changed from 20 to 300 msec (except at 50 pps).

The duration over which temporal integration occurs is very similar to that seen in the normal auditory system. The central origin of the normal auditory system's long-term temporal integration process is commonly acknowledged. Let us assume for the moment that a central temporal integrator is appropriate for modelling the long-term temporal integration process observed in these electrically stimulated patients. One commonly used model assumes that the central processor integrates neural activity over many fibers and over a time interval of approximately 100 to 300 msec and that the loudness function is some simple monotonic function of a single value which represents this total neural activity.

In this model, threshold and MCL are very sensitive functions of fiber recruitment. With fiber recruitment, we consider both the initial excitation of the fiber and the fiber's firing rate vs stimulus intensity function. Overall neural activity is determined by the number of recruited fibers and the firing rate of each of these recruited fibers. If at MCL, a large number of additional fibers are recruited (or perhaps equivalently, if the firing rates greatly increase) with only a small increase in stimulus amplitude, only a small increase in stimulus amplitude would be necessary to maintain the same quantity of « neural activity » for a large decrease in burst duration. If near threshold, only a small number of additional fibers are recruited for a relatively large increase in stimulus current, a relatively large incerase in stimulus current would be necessary to maintain the same « neural activity » for a given decrease in burst duration. Thus, if the recruitment function grew at an increasing rate with stimulus amplitude, we might expect MCL to be a weaker function of burst duration than threshold.

In contrast, if we assumed that the longer-term temporal integration occurred peripherally, then a two-population model could be proposed to account for the differences in threshold and MCL functions of burst duration. Such a model is very similar to that proposed in the previous section. These two hypothetical neural populations associated with long-term temporal integration would necessarily be distinctly different from the two hypothetical populations discussed in the previous section on short-

term temporal integration. The hypothetical « population A » short-term temporal integration neural processes are absent in subject C. However, both populations associated with long-term integration would be present in all three subjects.

Threshold and MCL as a function of pulse width and cycle duration

In all three subjects studied, thresholds dropped precipitously as pulse width was increased above 1-2 msec; and similarly, with sine wave stimuli, threshold decreased dramatically as the stimulus frequency was decreased below 500-1000 Hz. In contrast, a considerably smaller decrease in the MCL level was observed over these same stimulus ranges (Figs. 9 and 7). As a consequence, dynamic range is large for the larger pulse widths and for the lower frequency sine wave stimuli, particularly for sine wave stimuli in the 50-200 Hz range where dynamic ranges are 22-35 dB (see figure 10). Section 13 contains a discussion of some of the alternative mechanisms that may be responsible for the significant drop in threshold at the lower frequencies and larger pulse widths. Why does MCL not also drop as significantly as does threshold when the sinusoidal stimulus frequency is reduced below 200 Hz? Recording of single unit AVCN responses in cat to scala tympani electrical stimulation (White, 1983) has suggested one possible interpretation. Neural responses (Fig. 33) to sinusoidal stimuli of 100 and 200 Hz generally grew with stimulus amplitude at a considerably lower rate than did unit response to higher frequencies (i.e. 400 Hz, 3200 Hz, and 6400 Hz). This pattern was consistent for different stimulating electrodes and for different stimulus durations (i.e. 5, 20, and 80 msec stimulus durations). If the change in neural activity is less at 100 Hz and 200 Hz for a given change in stimulus intensity, then one might expect a more gradual loudness growth stimulus intensity and therefore an MCL higher than would have otherwise been expected at these low frequencies.

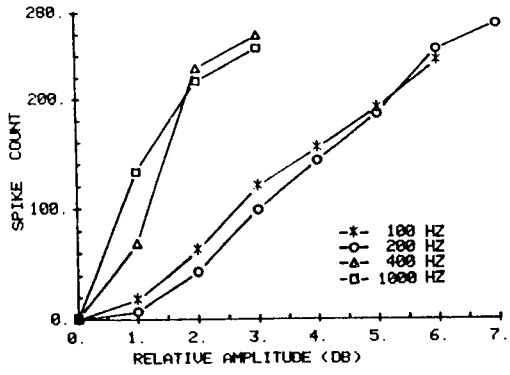

Fig. 33. - Spike counts for 100, 200, 400, and 3200-6400 Hz sinusoidal stimuli as a function stimulus amplitude (in dB) relative to threshold amplitude. Spike counts were obtained from the initial 20 msec response interval of unit recording in the large spherical cell region of the cat AVCN. Spike counts were obtained with 50 trials.

Stimulus duration

A number of investigators have focussed on threshold, loudness, and MCL functions for stimulus bursts of durations greater than 100 msec. The use of constant amplitude, long-duration sinusoidal stimuli for threshold, loudness, MCL, and intensity discrimination measurements is too limited a stimulus set for obtaining information useful in speech processor design. Relatively short transitions within the speech signal normally convey a large portion of speech information. These transitions range from a few msec to tens of milliseconds. Even the re-

latively « steady-state » portion of a vowel is quite complex in its envelope fluctuations. If the envelope is measured using anything but a very long integration period, the amplitude envelope of the vowel will vary considerably over time. The envelope is approximately periodic at the glottal period. This example illustrates how even the most « steady » segments of speech deviate considerably from the constant stimulus amplitude model that has often been used implicity. Stimulus is integrated over some interval of time. One component may be related to the nerve's hypothetical temporal integration. This component probably contributes significantly to changes in threshold over the first 20 msec of the stimulus, particularly when the pulse rate or stimulus frequency is above 200-400 Hz.

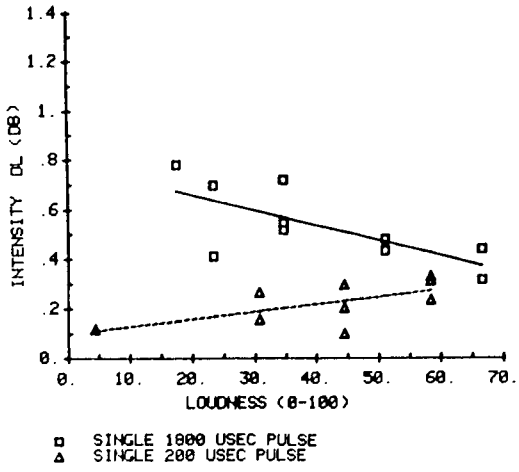

Fig. 34. - Intensity difference limens as a function of loudness for single pulses of 200 µsec and 1800 µsec pulse widths. Data is from subject B with bipolar electrode pair (7, 8) stimulated.

Mid-Range Functions

Intensity discrimination

In the normal auditory system, intensity discrimination as measured in dB is not a strong function of stimulus level. Sufficiently above threshold, intensity discrimination (measured in dB) may stay nearly constant or decrease by only a factor of 2 or 3 over an 80 dB change in stimulus level. Intensity dLs for normal hearing subjects may range from approximately 2 dB to .25 dB (Greenwood, 1983).

Intensity discrimination was measured as a funtion of burst duration, pulse rate, pulse amplitude,and pulse width for subject B. These intensity discrimination functions are a strong function of the subject. Preliminary results from a third subject (C) will be briefly reviewed and a comparison made.

Figure 34 illustrates how pulse width can affect the distribution of intensity dLs as a function of loudness for single pulses. Similarly, Figure 35 illustrates how pulse width affects the distribution of intensity dLs as a function of loudness for low repetition rate stimuli with burst durations of 300 msec. In both examples, the longer pulse width stimuli results in larger intensity dLs, particularly at the lower stimulus levels. The narrow pulse width stimuli produce relatively constant intensity dLs across the measured loudness range. The average intensity dL increases with pulse width as does the dynamic range (Figs. 8 and 25).

Figure 36 illustrates how pulse rate can affect the distribution of intensity dLs across the dynamic range. At low pulse rates, the intensity dL remains relatively constant with stimulus intensity. However, at high pulse rates, a marked change occurs in the distribution of intensity dLs across the dynamic range. At the low stimulus levels, a relatively large change in stimulus intensity is

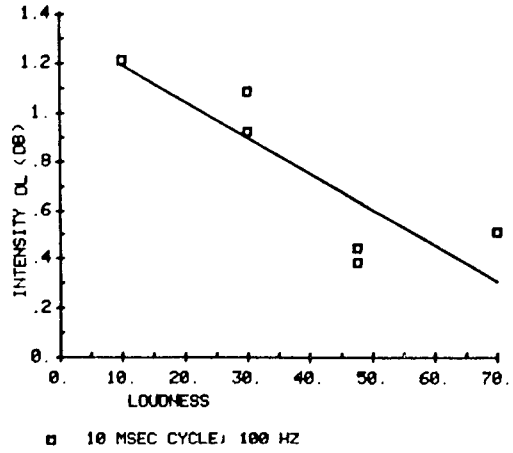

Fig. 35. - Intensity difference limens as a function of loudness for low repetition rate stimuli with a cycle duration 10 msec. Please compare this to that curve in figure 36 representing intensity dls for a small pulse width (200 μsec) and a low repetition rate (50 pps) with a burst duration of 300 msec. Burst duration was 300 msec. Data is from subject B with bipolar electrode pair (7, 8) stimulated.

necessary for discrimination. However, at the higher intensities, there is very little, if any, difference in the intensity dLs for the 50 pps and 2000 pps stimuli. The dynamic range for the high pulse rate stimuli is greater than the dynamic range for the low pulse rate stimulus (see figures 15 and 22) *and* correspondingly the average intensity dL for the high pulse rate stimulus is larger than the average intensity dL for the low pulse rate stimulus.

How does the intensity discrimination function change if the burst duration is changed ? Figure 37 illustrates intensity discrimination functions for two burst durations: a single 200 μsec pulse and a 2000 pps, 300 msec pulse train. Clearly, the functions are very different. With the single 200 μsec biphasic pulses, relatively constant and small intensity dLs are observed as com-

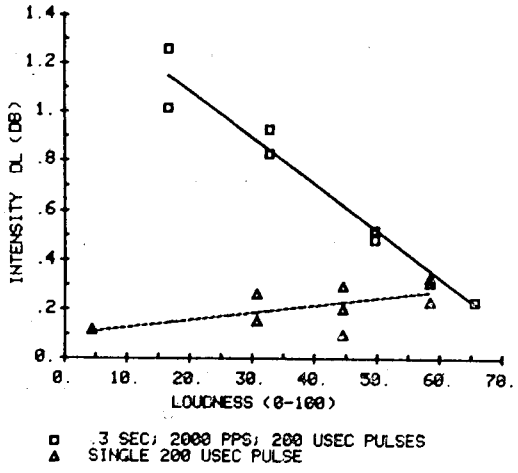

Fig. 36. - Intensity difference limens as a function of loudness for high pulse rate (2000 pps) vs low pulse rate (50 pps) biphasic, 200 μsec pulse trains of 300 msec duration. Data is from subjects B with bipolar electrode pair (7, 8) stimulated.

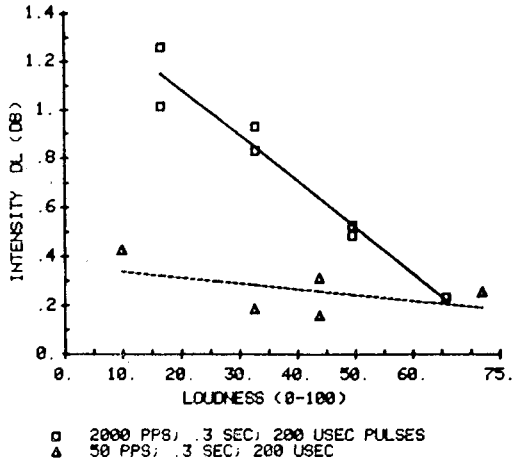

Fig. 37. - Intensity difference limens as a function of loudness for long burst duration (.3 sec, 2000 pps) and very short burst duration (one 200 μsec biphasic pulse) stimuli. Stimuli are composed of biphasic, 200 μsec pulses. Data is from subjects B with bipolar electrode pair (7, 8) stimulated.

pared to the large dLs observed for the 300 msec, 2000 pps stimuli at the lower stimulus intensities. As before, the stimulus which exhibited higher average intensity dLs also exhibited wider dynamic ranges (fig. 38).

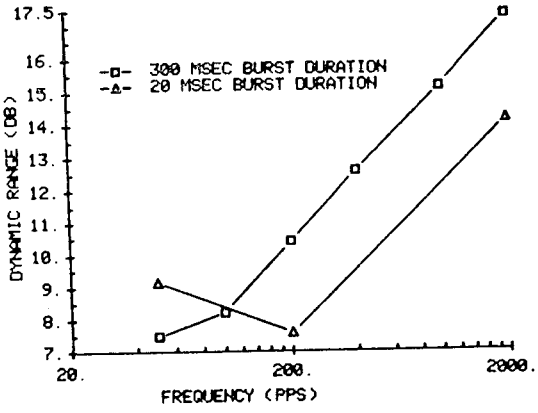

Fig. 38. - Dynamic range as a function of pulse rate for pulse trains of 20 msec and 300 msec in duration and a pulse width of 200 μsec. Data is from subject B with bipolar electrode pair (7, 8) stimulated.

Burst duration has a significant effect on the intensity dL and dynamic range functions if the pulse rate is sufficiently high. However, longer burst duration do not always increase intensity dLs. For example, Figure 39 illustrates just such a situation. In this case, the 300 msec stimulus is a 50 pps pulse train with the same pulse width as in the previous example. In this example, the distribution of intensity dLs across the dynamic range is relatively constant and approximately equal for both the single pulse and the 300 msec pulse train. Similarly, the dynamic ranges for the two stimuli are approximately equal (fig. 38).

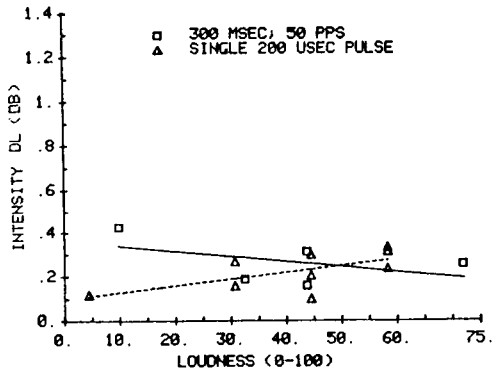

Fig. 39. - Intensity difference limens as a function of loudness for long burst duration (.3 sec, 50 pps) and very short burst duration (one 200 μsec biphasic pulse) stimuli. Stimuli are composed of biphasic, 200 μsec pulses. Data is from subject B with bipolar electrode pair (7, 8) stimulated.

In summary, either high pulse rate or large pulse width stimuli generated considerably elevated intensity dLs particularly at the lower stimulus intensities. For high pulse rate stimuli, as the burst duration was decreased the elevated intensity dLs (at the lower stimulus levels) decreased until the intensity dLs were equal to those of single pulses. Dynamic ranges were correspondingly higher for high pulse rate stimuli and large pulse width stimuli. Also, similarly the dynamic range for high pulse rate stimuli decreased as the burst duration was reduced.

Figure 40 illustrates how intensity discrimination and dynamic range co-vary for a range of stimuli in subjects A and B. Because the intensity discrimination and dynamic range measures co-vary in a reasonably consistent manner, we might expect that there are one or more common mechanisms involved in the generation of these two behavioral measures. In this figure, dynamic range has been calculated in a dif-

ferent manner than in the other illustrations. Dynamic range was calculated by subtracting the current level (in dB) required to obtain a loudness of 15 from that current level (in dB) required to obtain a loudness of 70. Current levels required to obtain specified loudnesses were determined with the « best-fit » equation described in section 2. (The cochlear prosthesis group at Stanford has used a similar method for a number of years.)

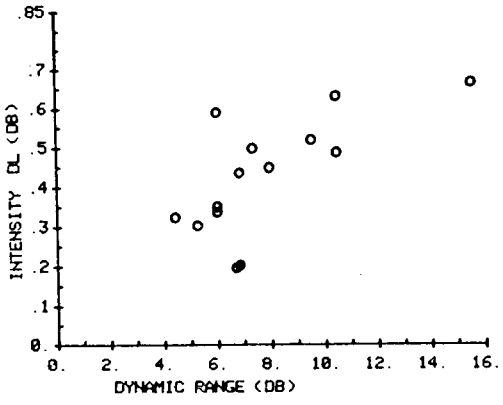

Fig. 40. - Scatter plot of two subject's (A and B) average intensity dLs as a function of dynamic range for a range of stimuli including biphasic pulse and sinusoidal stimuli at a set of burst durations. A « best-fit » line passing through these data points indicates that the average number of discriminable difference within the dynamic range may be in the order of 20.

As pulse rate or burst duration is increased, intensity dLs increase significantly particularly at the lower loudness levels. This may indicate that a change in pulse rate and/or burst duration has its primary effect on the fibers that are most sensitive to the stimulation. In a similar manner, an increase in pulse rate or burst duration reduces threshold considerably more (in dB) than the MCL (see Figures 13 and 9). In other words, *in subject B* intensity discrimination, threshold, and MCL measures indicate that changes in pulse rate and burst duration have their greatest effect on the lower regions of the dynamic range.

There are a number of factors that may influence intensity discrimination across the dynamic range. This is a partial list of those factors:

(1) The number of additional fibers excited for a given increment in stimulus intensity. Such « recruitment » is a function of the current spread around the stimulating electrodes and the density of excitable neural processes. Such « recruitment » is a function of « the current density as a function of location » and « the density of excitable neural processes as a function of location within the cochlea and modiolus ».

(2) The rate at which the firing rate increases for a given increment in stimulus intensity.

(3) If their are two or more populations which demonstrate different responses to a stimulus variable, then the intensity discrimination function could be significantly affected due to such a response differential.

Loudness functions

Figure 41 displays loudness as a function of stimulus amplitude for pulses with short and long burst durations. If the stimulus amplitude is displayed on a log scale, the loudness functions grow slowly at first and then increase very significantly as the stimulus is increased further. If the stimulus amplitude is displayed on a linear scale, the loudness functions appear to grow more linearly. Loudness functions were well fit

with a simple equation of the form: (a+bI)**c, in which a, b, and c are constants for a given stimulus and « I » is the stimulus amplitude in μamp. These curve fitting were used to obtain estimates of the current levels required to obtain a loudness of '15' and a loudness of '70' in order to calculate a more conservative estimate of the subjects' dynamic range (see previous section).

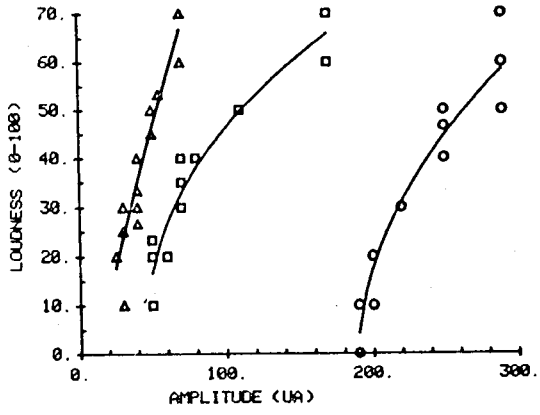

Fig. 41. - Loudness as a function of stimulus amplitude for three types of stimuli: a single 200 μsec biphasic pulse (circles); a 300 msec, 2000 pps pulse train of 200 μsec biphasic pulses (squares); and a single 1800 μsec biphasic pulse (triangles). Loudness function were well fit with a simple equation of the form: (A+Bx)**C, where A, B, and C are constants for a given stimulus. Data is from subject B with bipolar electrode (7, 8) stimulated.

Variation of Loudness

In both subjects A and B, loudness estimates at the lower stimulus levels varied with a standard deviation of about +/— 10 units on the 0 to 100 loudness scale. The standard deviation of the loudness estimates decreased as a function of the mean loudness. This variability was particularly troublesome, at loudness levels below 10 to 20 on the loudness scale. In many instances, the stimulus that « on the average » would elicit a loudness estimate of « 10 » would be inaudible to the subject. As a consequence, intensity discrimination and pitch measurements at average loudness levels of « 10 » and « 20 » on the loudness scale were more difficult. More significant, is the effect of such variability on speech and sound processor design. For example, one would probably want to design processors in such a manner that all significant stimuli are placed sufficiently above threshold to insure that the sounds will nearly always be audible. In effect, this means that the designer has less useful dynamic range to work with.

Why is there such variability at these low levels? There are probably a number of reasons. One suggestion involves a tinnitus or head noise. These subject-described « head noises » vary in their intensity over time and were present both before and after the implantation of the electrode array. This form of « tinnitus » may act as an effective masker of the lower stimulus levels.

Subject A exhibited another, perhaps related, characteristic in her loudness estimates. When listening to repetitive 300 msec stimulus bursts (with a 700 msec inter-stimulus interval), subject A reported that the loudness of these constant amplitude bursts varied over a considerable range during a listening interval. More specifically, the loudness estimates would wax and wane over 30-40% of the dynamic range. Sudden loudness changes did not occur; but the bursts were said to slowly change in loudness. Both a midrange stimulus (approximately 50 loudness units on the average) and a lower level stimulus (approximately

20-30 units « on the average ») were investigated. Only an approximate description of this process can be attempted here. The maximum rate of change of these loudness estimates was approximately 10 loudness units for a 3-5 sec interval. More typically, subject A's estimates would change about 10 loudness units within a 5 to 15 sec interval. This characteristic of subject A's estimates was observed during three separate test sessions over a two week period.

In contrast, subject B heard the repeating constant amplitude stimulus bursts as a set of constant loudness bursts.

Multichannel stimulation

Previous work on electrode interactions has been reported. Suffice it to say, that a large body of work is necessary to design multichannel processors that efficiently map perceptually significant acoustic information into electrical stimuli across a multichannel array. Previous studies (White, 1983; Eddington, 1978; and Merzenich and White, 1976) have presented evidence that electric field interactions may occur during electrical stimulation of two or more channels. White (1982) and Herndon (1982) have presented evidence that temporal interactions occur between two channels. One design strategy has been to avoid these interactions by using a set of techniques described below. However, with a better understanding of these interactions, it may be possible to effectively utilize them to expand and improve the transmission of useful information to the nervous system.

One method used to minimize these channel interactions, is to minimize the distance between the electrodes and the excitable tissue. Also, the distance between the electrode channels may be increased to avoid these interactions. Still another technique may be useful: that of temporally interlacing the stimuli on the channels. This technique avoids the electric field interactions that occur when simultaneously stimulating two or more channels. Non-simultaneous stimulation appears to very significantly reduce channel interactions. However, this technique alone does not eliminate « temporal » interactions. The nerve membrane appears to partially summate excitation over a post-stimulus time interval of 2-5 msec in some subjects. Stimuli from two channels may partially summate at the nerve even when the stimuli are not temporally overlapping. However, if the stimuli are separated in time by at least 4-10 msec, these interactions are significantly reduced. A combination of the above techniques may be useful in reducing channel interactions.

In the design of proposed speech or sound processors, it is important to estimate the range of stimuli that will appear at the cochlear electrodes. Some processors may use only biphasic pulse stimuli over a restricted set of pulse widths, rates, and amplitudes. Because such a stimulus set is restricted, stimulus processing may be correspondingly simpler. Other processors may use what is commonly refered to as « analog » stimuli. The term « analog » is ill-defined, but generally implies that the stimulus at the electrodes is continuously varying in time and that the spectral content of the stimulus is generally within the typical speech range of 200 to 8 KHz. Generally, the « analog » stimulus is some derivative of the original acoustic speech signal.

After the range of stimuli have been estimated, it is hoped that the prosthesis designer can use the concepts and data presented in this manuscript to help in his design of a cochlear prosthesis.

RIASSUNTO

L'A. effettua una analisi psicoacustica della funzione di discriminazione per soglia, 'loudness' e intensità adoperando una vasta gamma di stimoli.

Per l'interpretazione dei dati comportamentali, sviluppa dei modelli fenomenologici per tali funzioni, servendosi di concetti neurofisiologici fondamentali tra cui i processi di integrazione temporale.

Presenta dei dati comparativi sugli impianti cocleari uni- e multicanale in modo che il progettista possa approfondire meglio le conseguenze della stimolazione elettrica del nervo acustico.

REFERENCES

BUTIKOFER, R., and LAWRENCE, P. D. (1979) Electrocutaneous nerve stimulation - II: stimulus waveform selection. *IEEE Transactions Biomedical Engineering, 26,* 69.

CLOPTON, B. M., SPELMAN, F. A., and MILLER J. M. (1980) Estimates of essential neural elements for stimulation through a cochlear prosthesis. *Annals of Otology, Rhinology and Laryngology, 89,* suppl. 66, 5.

EDDINGTON, D. K., DOBELLE, W. H., MLADEJOVSKY, M. G., BRACKMANN, D. E., and PARKIN, J. L. (1978) Auditory prosthesis research with multiple channel intracochlear stimulation in man. *Annals of Otology, Rhinology and Laryngology, 87,* suppl. 53, 5.

FOURCIN, A. J., ROSEN, S. M., MOORE B. C. J., DOUEK, E. E., CLARK, G. P., DODSON, H., and BANNESTER, L. H. (1979) External electrical stimulation of the cochlea: clinical, psychophysical, speech-percentual, and histological findings. *British Journal of Audiology, 13,* 85.

FRANKENHAEUSER, B., and HUXLEY, A. F. (1964) The action potential in the myelinated nerve fiber of Xenopus Laevis as computed on the basis of voltage clamp data. *Journal of Physiology, 171,* 302.

GREEN, D. M., and SWETS J. A. (1974) *Signal detection theory and psychophysics.* John Wiley and Sons 1966, reprinted by R. E. Krieger Publ. Co., New York.

HERNDON, M. K. (1981) *Psychoacoustics and speech processing for a modiolar auditory prosthesis.* Technical Report No. G906-5; Stanford Electronics Laboratories, Stanford University, Stanford, CA.

HILL, A. V. (1936a) Excitation and accomodation in nerve. *Proceedings of the Royal Society, 119,* 305.

HILL, A. V., KATZ, B., and SOANDT, D. Y. (1936b) Nerve excitation by alternating current. *Proceedings of the Royal Society, 121,* 74.

HOCHMAIR-DESOYER, I. J., HACHMAIR, E. S., FISCHER, R. E., and BURIAN, K. (1980) Cochlear prosthesis in use: recent speech comprehension results. *Archives of Otolaryngology, 229,* 81.

HODGKIN, A. L., and HUXLEY, A. F. (1952) A quantitative description of membrane current and it application to conduction and excitation in nerve. *Journal of Physiology, 117,* 500.

KIANG, N. Y. S., and MOXON, E. C. (1972) Physiological considerations in artificial stimulation of the inner ear. *Annals of Otology, Rhinology and Laryngology, 81,* 714.

LEVITT, H. (1971) Transformed up-down methods in psychoacoustics. *Journal of the Acoustical Society of America, 49,* 467.

LOEB, G. E., WHITE, M. W., and JENKINS, W. M. (1983) Biophysical Considerations in Electrical Stimulation of the Auditory Nervous System. *Annals of the New York Academy of Sciences* (in press).

LOEB, G. E., BYERS, C. L., REBSCHER, S. J., CASEY, D. E., FONG, M. M., SCHINDLER, R. A., GRAY, R. F., and MERZENICH, M. M. (1983) Design and fabrication of an experimental cochlear prosthesis. *Medical and Biological Engineering and Computing, 21,* 241.

LOEB, G. E., WHITE, M. W., and MERZENICH, M. M. (1983) A new theory of acoustic pitch perception. *Biological Cybernetics* (in press).

MCNEAL, D. R. (1976) Analysis of model for excitation of myelinated nerve. *IEEE Transactions of Biomedical Engineering, 23,* 329.

MCNEAL, D. R., and TEICHER, D. A. (1977) *Effect of electrode placement on threshold and initial site of excitation of a mylenated nerve fiber.* In: Resnick, J., Hambrech, T.: *Functional electrical stimulation.* New York, M. Dekker.

MERZENICH, M. M., MICHELSON, R. P., PETTIT, C. R., SCHINDLER, R. A., and REID, M. (1973) Neural encoding of sound sensation evoked by electrical stimulation of the acoustic nerve. *Annals of Otology, Rhinology and Laryngology, 82,* 486.

MORAN, N., and PALTI, Y. (1980) Potassium ion accumulation at the external surface of the nodal membrane i nfrog myelinated fibers. *Biophysical Journal, 32,* 939.

SIMMONS, F. B. (1966) Electrical stimulation of the auditory nerve in man. *Archives of Otolaryngology, 84,* 1.

SIMMONS, F. B., WHITE, R. L., MATHEWS, R. G., and WALKER, M. G. (1981) Pitch correlates of direct auditory nerve electrical stimulation. *Annals of Otology, Rhinology and Laryngology, suppl. 82,* 15.

SPELLMAN, F. A., CLOPTON, B. M., and PFINGST, B. E. (1982) Tissue impedance and current flow in the implanted ear. *Annals of Otology, Rhinology and Laryngology, suppl., 91,* 3.

TEICHER, D. A., and MCNEAL, D. R. (1978) Comparison of a dynamic and steady-state models for determining nerve fiber threshold. *IEEE Transactions of Biomedical Engineering 25,* 105.

VERVEEN, A. A. (1959) *On the fluctuation of threshold of the nerve fiber.* In: Tower, D. B., Schadde, J. J.: *Structure and Function of the General Cortex.* Proceedings of the Second International Meeting of Neurobiologists, Amsterdam.

VUREK, L. S., WHITE, M. W., FONG, M., and WALSH, S. M. (1981) Opto-isolated stimulators used for electrically evoked BSER. *Annals Otology Rhinology and Laryngology, suppl. 82,* 21.

WHITE, M. (1978) *Design Considerations of a Prosthesis for the Profoundly Deaf.* Doctoral Dissertation, University of California, Berkeley.

WHITE, M. W., MERZENICH, M. M., and LOEB, G. E. (1983) Electrical stimulation of the eighth nerve in cat: Temporal properties of unit responses in the large spherical cell region of the AVCN. *Annals of Otology, Rhinology and Laryngology* (submitted).

WHITE, M. W., MERZENICH, M. M., and GARDI, J. N. (1983) Multichannel electrical stimulation of the auditory nerve: channel interaction and processor design. *Archives of Otolaryngology* (submitted).

M. W. WHITE, ~~M.D.~~

School of Medicine
Department of Otolaryngology
University of California
San Francisco, California
94143 (USA)